Safe Barrier-Constrained Control of Uncertain Systems via Event-triggered Learning

Armin Lederer*, *Member, IEEE*, Azra Begzadić*, *Graduate Student Member, IEEE,* Sandra Hirche, *Fellow, IEEE,* Jorge Cortés, *Fellow, IEEE,* Sylvia Herbert, *Member, IEEE*

***Abstract*— While control barrier functions are employed in addressing safety, control synthesis methods based on them generally rely on accurate system dynamics. This is a critical limitation, since the dynamics of complex systems are often not fully known. Supervised machine learning techniques hold great promise for alleviating this weakness by inferring models from data. We propose a novel control barrier function-based framework for safe control through event-triggered learning, which switches between prioritizing control performance and improving model accuracy based on the uncertainty of the learned model. By updating a Gaussian process model with training points gathered online, the approach guarantees the feasibility of control barrier function conditions with high probability, such that safety can be ensured in a data-efficient manner. Furthermore, we establish the absence of Zeno behavior in the triggering scheme, and extend the algorithm to sampled-data realizations by accounting for inter-sampling effects. The effectiveness of the proposed approach and theory is demonstrated in simulations.**

***Index Terms*— Event-triggered learning, safety-critical control, Gaussian processes, control barrier functions.**

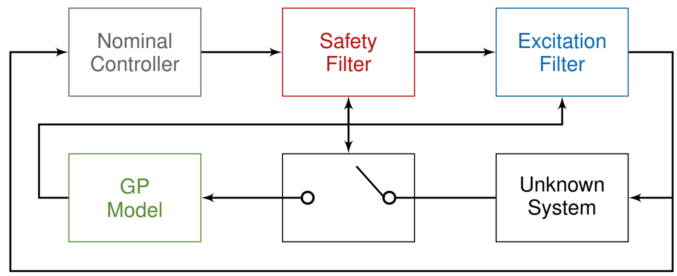

Fig. 1. Overview of the proposed approach for safe learning-based control synthesis through event-triggered learning with Gaussian processes and control barrier functions. A nominal controller (grey) passes through a safety filter (red) constructed using a CBF and GP model (green), which minimally modifies the control to ensure safety. When the model uncertainty becomes too high, an update event is triggered, which activates the excitation filter (blue) to generate sufficiently informative data used to update the GP model. Otherwise, the nominal control law is only adapted by a safety filter, which relies on the GP model.

I. Introduction

Control barrier functions (CBFs) are commonly used to guarantee the safety of nonlinear systems. Given a valid CBF for a control-affine nonlinear system, safe control inputs can be efficiently synthesized online using a quadratic program (QP). However, this QP formulation generally assumes perfect knowledge of system dynamics, which can be challenging to derive analytically for many applications. For example, real-world systems such as autonomous vehicles, industrial machinery, and medical robots have inherent complexity, which often prevents accurate system identification using classical techniques. Recently, Gaussian processes (GPs) have gained attention for system identification in control due to their strong theoretical foundations [1]. GPs generalize well due to their ability to make accurate predictions even with a small amount of data. Moreover, they are particularly well suited for safety-critical problems since they provide a measure of model uncertainty along with their predictions, which allows the derivation of prediction error bounds [2], [3]. Therefore, CBFs in combination with GPs hold a great promise for the safe control of uncertain systems [4]–[6]. This paper introduces a novel CBF-based framework for ensuring sampled-data safety and recursive feasibility guarantees through event-triggered learning with GPs for systems under uncertain, nonlinear input perturbations. As outlined in Fig. 1, our approach modifies a nominal control law via a CBF-based safety filter, which is defined using a GP model of the unknown dynamics. This safety filter step can be formulated as a second-order cone program (SOCP), which is known to lack feasibility guarantees in general, see e.g. [7], [8]. Therefore, we derive a novel, straightforwardly interpretable condition for the existence of admissible control inputs. By requiring a sufficiently large ratio between the GP's mean and standard deviation, our feasibility condition ensures that learning errors do not dominate the nominal model, thereby effectively ensuring a form of 'robust controllability'. Using this condition, we show that the CBF-based safety filter can be implemented as a QP despite the lack of an exact model.

Since it can be hard to guarantee the satisfaction of the feasibility condition using offline data, we design an event trigger which updates the GP model using data generated online. To ensure a sufficient increase in model accuracy, we

* *Armin Lederer and Azra Begzadić contributed equally to this work.*
A. Lederer is with the Learning and Adaptive Systems Group, Department of Computer Science, ETH Zurich, Switzerland (e-mail: armin.lederer@inf.ethz.ch).
A. Begzadić, J. Cortés and S. Herbert are with the Department of Mechanical and Aerospace Engineering, University of California, San Diego (e-mail: abegzadic@ucsd.edu, cortes@ucsd.edu, sherbert@ucsd.edu).
S. Hirche is with the Chair of Information-oriented Control, TUM School of Computation, Information and Technology, Technical University of Munich, Germany (e-mail: hirche@tum.de).

derive a finite, closed-form, lower bound for the necessary control inputs in the generated training data set. We exploit this knowledge in an excitation filter, which suitably scales control inputs in a safe direction when a model update is triggered. Thereby, our event-triggered learning approach ensures the recursive feasibility of the CBF constraints and consequently the safety of the control system.

In order to further facilitate the real-world implementability of the proposed control scheme, we extend it to a sampled-data realization by tightening the CBF constraints in dependence on the sampling time. We show that the inter-event time is lower bounded by a positive value, such that the occurrence of Zeno behavior [9], [10], i.e., an infinite number of trigger events in a finite time interval, is excluded. This lower bound allows us to account for inter-sampling effects in the event trigger via an early triggering strategy. Thereby, safety and feasibility guarantees from the continuous-time analysis are maintained despite a sampled-data realization of the control law.

The remainder of this article is structured as follows: Section II defines the problem formulation. In Section III, we present a novel event-triggered learning approach with a switching control law that guarantees safety and feasibility. The extension of this approach to sampled-data systems is proposed in Section IV. Finally, in Section V, we illustrate the proposed methods in numerical simulations to demonstrate its effectiveness in an adaptive cruise control example, before we conclude the paper in Section VI.

Related Work: When the effect of the control input on the dynamics is known, GP accuracy guarantees can be directly employed for adapting the robustness of CBF conditions to the model error [4]. By reflecting control-affine model structures in the kernel used in GPs, this adaptation strategy can be straightforwardly extended to obtain safe control inputs despite model uncertainty [5], [6]. Since the resulting optimization problems for determining control inputs become SOCPs rather than QPs, safety can be efficiently ensured in principle.

However, these guarantees are limited to an idealized setting which ignores challenges we are confronted with in the execution of the control law: 1) computation times requiring a discrete-time realization of controllers, and 2) the feasibility of the CBF constraints, potentially in combination with control input constraints. The discrepancy between continuous-time derivation of safety guarantees and a practical implementation in discrete time can be straightforwardly dealt with in the absence of a GP model. For example, the inter-sampling effects arising from discretizations such as zero-order hold (ZOH) can be considered in the CBF conditions through a safety margin [11]. By basing these safety margins on a local Lipschitz analysis, the conservativeness of tightening the CBF constraints in sampled-data realizations is reduced [12]. Even though it is possible to extend these ideas to approaches ensuring safety using CBFs and offline trained GP models [13], the feasibility of the resulting optimization problem is not guaranteed.

This loss of feasibility guarantees comes from the SOCP structure that is required due to model uncertainties; feasibility guarantees are not directly inherited from the original QP formulation and strongly depend on the uncertainty of the employed GP model [7], [8]. Due to the inherent relationship between model uncertainty and the available training data, the feasibility of the CBF constraint is crucially influenced by the data generation approach. This insight motivates the application of online learning strategies to ensure feasibility. In particular, event-triggered learning [14] is a promising paradigm wherein data is collected and the model is updated only when certain conditions are satisfied, e.g., model uncertainty exceeds a prescribed threshold. Event-triggered learning applied to GP model inference is exploited for Lyapunov-based stabilization [15], [16], for which exceptional data efficiency is demonstrated. Due to the close relationship between Lyapunov functions and barrier functions [17], it is possible to extend these concepts to CBFs. While first results [18], [19] have shown the efficacy of this approach in ensuring feasibility when directly learning the CBF constraint, they exhibit crucial weaknesses. Their feasibility guarantees potentially require the application of arbitrarily large control inputs when GP updates are triggered, rendering the theoretical analysis void when considering input constraints. Moreover, Zeno behavior cannot be excluded, such that a transfer of guarantees for the theoretically analyzed continuous-time control law to discrete-time implementations is not straightforward. Even though some issues such as the potentially unbounded control inputs are mitigated through extended data generation phases [20], this strategy exhibits other weaknesses, e.g., arbitrarily poor control performance when gathering data. Therefore, providing sampled-data feasibility and safety guarantees for GP-based CBF approaches remains an open problem.

II. Problem Formulation and Preliminaries

A. Notation

Vectors and matrices are denoted by bold lower and upper-case symbols, respectively. We denote by $\mathbb{R}_{>0}$ and $\mathbb{R}_{\geq 0}$ the sets of real positive numbers without and with zero, respectively, and by $\mathbb{N}$ the set of natural numbers. The Euclidean norm is denoted by $\|\cdot\|$. A function $f : \mathbb{R}^n \to \mathbb{R}$ is locally Lipschitz if, for every compact set $\mathcal{S} \subset \mathbb{R}^n$, there exists $L > 0$ such that $\|f(x) - f(y)\| \leq L\|x - y\|$, for all $x, y \in \mathcal{S}$. $\nabla_{\boldsymbol{x}} f$ denotes the gradient of a function f with respect to $\boldsymbol{x}$. A continuous function $\alpha : \mathbb{R}_{>0} \to \mathbb{R}_{>0}$ is of extended class $\mathcal{K}$ function if it is strictly increasing, $\alpha(0) = 0$, $\lim_{r\to\infty} \alpha(r) = \infty$ and $\lim_{r\to-\infty} \alpha(r) = -\infty$. The Gaussian distribution with mean $\mu \in \mathbb{R}$ and variance $\sigma^2 \in \mathbb{R}_{>0}$ is denoted by $\mathcal{N}(\mu, \sigma^2)$. The function $\mathrm{diag}([x_1, x_2, \dots x_n])$ constructs a diagonal matrix where the elements $(x_1, x_2, \dots x_n)$ are scalar values representing the diagonal entries, with all off-diagonal elements being zero. $\boldsymbol{I}_N$ denotes the $N \times N$ identity matrix. $\boldsymbol{x'} \in \mathbb{R}^n$ denotes the test point. The absolute value of a scalar value x is denoted by $|x|$. The sign function, denoted as $\mathrm{sign}(\cdot)$, is defined to return -1 for negative values, 0 for zero, and 1 for positive values.

B. Problem Setting

We consider single-input linear dynamical systems with nonlinear input perturbation of the form

$$\dot{\boldsymbol{x}} = \boldsymbol{A}\boldsymbol{x} + \boldsymbol{b}(f(\boldsymbol{x}) + g(\boldsymbol{x})u) \tag{1}$$

with state $\boldsymbol{x} \in \mathcal{X} \subseteq \mathbb{R}^n$ and input $u \in \mathcal{U} \subseteq \mathbb{R}$, where $\mathcal{U}$ and $\mathcal{X}$ are compact sets. Throughout the paper, the argument t in $\boldsymbol{x}(t)$ and $u(t)$ is omitted for brevity whenever possible. While the matrix $\boldsymbol{A} \in \mathbb{R}^{n\times n}$, vector $\boldsymbol{b} \in \mathbb{R}^n$, and the control-affine structure of the dynamics are assumed to be known, the functions $f : \mathcal{X} \to \mathbb{R}$ and $g : \mathcal{X} \to \mathbb{R}$ are considered unknown. This structure covers a wide range of system classes that can be represented by input-affine nonlinear systems in canonical form, such as Euler-Lagrange models, where $\boldsymbol{A}$ reflects an integrator structure.

Remark 1: The restriction to systems with scalar inputs is only used for notational convenience in subsequent sections, but all results straightforwardly extend to multi-input systems with block-diagonal matrix $\boldsymbol{B}$ and diagonal matrix $\boldsymbol{G}(\boldsymbol{x})$.

To ensure that (1) is a well-behaved dynamical system, we pose additional requirements on the unknown functions $f(\cdot)$ and $g(\cdot)$, which are formalized in the following assumption.

Assumption 1: The unknown functions $f(\cdot)$ and $g(\cdot)$ are locally Lipschitz continuous on the compact domain $\mathcal{X}$, with Lipschitz constants L_f and L_g, respectively.

Assumption 1 ensures existence of a unique solution to the system (1) and can commonly be found in the literature of nonlinear control [21]. Moreover, this assumption is commonly satisfied for a wide range of systems. Thus, Assumption 1 is generally not restrictive.

Remark 2: Assumption 1 directly implies that there exist lower bounds $\underline{f}$, $\underline{g}$ and upper bounds $\bar{f}$, $\bar{g}$ for $f(\boldsymbol{x})$, $g(\boldsymbol{x})$ on the compact domain $\mathcal{X}$, i.e.,

$$\underline{f} \leq f(\boldsymbol{x}) \leq \bar{f}, \tag{2a}$$

$$\underline{g} \leq g(\boldsymbol{x}) \leq \bar{g}, \tag{2b}$$

for all $\boldsymbol{x} \in \mathcal{X}$.

Based on this system description, we consider the problem of designing a control law $\pi : \mathcal{X} \to \mathbb{R}$ which ensures the safety of the system (1). The primary goal of safety is to constrain all system trajectories to a predefined safe set $\mathcal{C}$, which we assume to exhibit no isolated points. We define this set as the zero-super level set $\mathcal{C} = \{\boldsymbol{x} \in \mathcal{X} : \psi(\boldsymbol{x}) \geq 0\}$ of a continuously differentiable function $\psi : \mathcal{X} \to \mathbb{R}$. Therefore, safety essentially reduces to forward invariance of $\mathcal{C}$, as formalized in the following definition.

Definition 1 (Safety): A system (1) is safe with respect to the set $\mathcal{C}$ if this set is forward control invariant, i.e., for some $u \in \mathcal{U}$ starting at any initial condition $\boldsymbol{x}_0 \in \mathcal{C}$, it holds that $\boldsymbol{x}(t) \in \mathcal{C}$ for $\boldsymbol{x}(0) = \boldsymbol{x}_0$ and all $t \geq 0$.

A common method to show this form of safety relies on the concept of barrier function (CBF), a powerful tool to certify the safety of a wide range of control laws.

Lemma 1 (Control Barrier Functions [17]): Consider a dynamical system (1) and a set $\mathcal{C}$ defined by a continuously differentiable function $\psi : \mathcal{X} \to \mathbb{R}$. If there exists an extended class $\mathcal{K}_\infty$ function $\alpha : \mathbb{R} \to \mathbb{R}$ such that

$$\max_{u\in\mathcal{U}} c(\boldsymbol{x}) + d(\boldsymbol{x})u \geq 0, \tag{3}$$

with

$$c(\boldsymbol{x}) = \nabla_{\boldsymbol{x}}^T \psi(\boldsymbol{x})(\boldsymbol{A}\boldsymbol{x} + \boldsymbol{b}f(\boldsymbol{x})) + \alpha(\psi(\boldsymbol{x})), \tag{4a}$$

$$d(\boldsymbol{x}) = \nabla_{\boldsymbol{x}}^T \psi(\boldsymbol{x})\boldsymbol{b}g(\boldsymbol{x}), \tag{4b}$$

holds for all $\boldsymbol{x} \in \mathcal{C}$, $\psi(\cdot)$ is called *control barrier function* (CBF) and every Lipschitz control law $\pi(\cdot)$ such that $\pi(\boldsymbol{x}) \in \{u \in \mathcal{U} : c(\boldsymbol{x}) + d(\boldsymbol{x})u \geq 0\}$ renders the system (1) safe with respect to $\mathcal{C}$.

The crucial component necessary for the application of this result is access to a valid CBF. Our work does not focus on the construction of CBFs, but rather on exploiting them to ensure safety with event-triggered learning. Hence, we make the following assumption.

Assumption 2: A twice differentiable CBF $\psi(\cdot)$ and a Lipschitz continuous extended class $\mathcal{K}_\infty$ function $\alpha(\cdot)$ satisfying the conditions of Lemma 1 are known for system (1) with $f(\boldsymbol{x}) = 0$ and $g(\boldsymbol{x}) = 1$. This CBF induces a compact control invariant set $\mathcal{C} = \{\boldsymbol{x} \in \mathcal{X} : \psi(\boldsymbol{x}) \geq 0\}$.

While the construction of CBFs for nonlinear systems can be challenging, Assumption 2 only requires us to find a suitable CBF for a linear dynamical system, which significantly simplifies the problem. For example, when $\boldsymbol{A}$ reflects an integrator structure, suitable CBFs can be iteratively constructed using the approaches proposed in [22], [23]. Therefore, Assumption 2 is generally not restrictive. Note that this assumption does not require knowledge of the unknown functions $f(\cdot)$ and $g(\cdot)$. Instead, other works [13], [18], [24] require knowledge of a CBF for the unknown system, which belongs to a more general class than the ones considered here.

To ensure that the CBF considered in Assumption 2 for $f(\boldsymbol{x}) = 0$, $g(\boldsymbol{x}) = 1$ also satisfies the conditions of Lemma 1 for arbitrary, unknown functions $f(\cdot)$, $g(\cdot)$, we make the following assumption.

Assumption 3: The unknown function $g(\cdot)$ is lower bounded by a positive scalar $\underline{g} \in \mathbb{R}_{>0}$, i.e., $g(\boldsymbol{x}) \geq \underline{g}$ for all $\boldsymbol{x} \in \mathcal{X}$.

This assumption does generally not impose strong requirements on $g(\cdot)$. The lower bound $\underline{g}$ is positive for many classes of dynamical systems such as mechanical systems, where $g(\cdot)$ is related to the inertia. If we knew $f(\cdot)$ and $g(\cdot)$, these assumptions would allow us to immediately define a safety filter

$$u^*(x) = \arg\min_{u\in\mathbb{R}} \|\pi_{\text{nom}}(\boldsymbol{x}) - u\|^2 \tag{5a}$$

$$\text{s.t. } c(\boldsymbol{x}) + d(\boldsymbol{x})u \geq 0 \tag{5b}$$

which minimally modifies a given nominal control law $\pi_{\text{nom}} : \mathcal{X} \to \mathbb{R}$, such that (3) can be straightforwardly ensured. Under sufficient smoothness of $\alpha(\cdot)$, $\psi(\cdot)$ and $\pi_{\text{nom}}(\cdot)$, the resulting control law can even be shown to be locally Lipschitz continuous [17], such that Lemma 1 ensures the safety of the closed-loop system. However, this approach is not directly applicable in a setting where $f(\cdot)$ and $g(\cdot)$ are unknown.

In order to overcome this limitation, we assume the ability to collect data online such that we can learn models $\hat{f} : \mathcal{X} \to \mathbb{R}$ and $\hat{g} : \mathcal{X} \to \mathbb{R}$ using GP regression. For this data, we require the following properties.

Assumption 4: At arbitrary sampling times $t \in \mathbb{R}_{\geq 0}$, training data $([\boldsymbol{x}^T(t), u(t)]^T, y(t))$ with outputs $y(t) = f(\boldsymbol{x}(t)) + g(\boldsymbol{x}(t))u(t) + \omega_t$ perturbed by i.i.d. Gaussian noise $\omega_t \sim \mathcal{N}(0, \sigma_{\text{on}}^2)$, $\sigma_{\text{on}}^2 \in \mathbb{R}_{>0}$, can be collected.

To be able to realize event-triggered learning strategies, it is common to allow sampling at arbitrary sampling times as previously already assumed, e.g., in [15]. Assumption 4 requires noise-free state measurements, while training targets y can be perturbed by Gaussian noise, which is a frequently used assumption in the GP-based control literature [25], [26]. In fact, noise-free measurements are often a prerequisite for analyzing continuous-time controllers [21]. Hence, we restrict our attention to noise-free states to streamline the presentation, even though the extension to noisy state measurements is possible under certain assumptions [27].

While Assumption 4 allows the generation of data by applying a control input for an infinitesimal amount of time, this is not possible with controller implementations running on computers with fixed sampling rate. Therefore, we additionally need to consider the effects of applying control inputs only at discrete times t_k, i.e.,

$$u\left(t\right)=\pi(\boldsymbol{x}(t_k)),\quad \forall t\in[t_k,t_{k+1}) \tag{6}$$

with $t_k=kT$ for all $k\in\mathbb{N}$, such that it becomes necessary to analyze a sampled-data system.

Based on this system description and Assumptions 1-4, we consider the problem of designing a sampling strategy to determine when measurements need to be taken and a sampled-data control law $\pi(\cdot)$, such that safety as defined in Definition 1 is guaranteed. Since this is a challenging problem, we first address this problem for continuous-time systems in Section III. In Section IV, we extend the results to consider the effects of the restriction to control laws of the form (6) to enable safe online learning in sampled-data systems.

III. Safe Control through Event-Triggered Learning

In this section, we address the problem of designing an event-triggered learning scheme together with a switching control law to provide safety. We first introduce the fundamentals of Gaussian process regression in Section III-A. In Section III-B, we demonstrate how control-affine system models can be inferred from data along with prediction error bounds based on GPs. Based on these GP models, we provide a QP-based approach for synthesizing safe control laws in Section III-C. We use this control law as a basis for the design of a switching controller and an event-triggered learning approach, which we prove to guarantee safety under weak assumptions in Section III-D. The guarantees for the exclusion of Zeno behavior with the proposed event trigger are given in Section III-E.

A. Gaussian Process Regression

Gaussian process regression (GPR) is a statistical method based on the concept that any finite number of measurements $\{h(\boldsymbol{q}^{(1)}),\ldots,h(\boldsymbol{q}^{(N)})\}$, $N\in\mathbb{N}$, of an unknown function $h:\mathcal{Q}\to\mathbb{R}$ evaluated at $\boldsymbol{q}\in\mathcal{Q}$ from some index set $\mathcal{Q}$, e.g., $\mathcal{Q}=\mathbb{R}^n$, follows a joint Gaussian distribution. A GP, denoted $h(\cdot)\sim\mathcal{GP}(\hat{h}(\cdot),k_h(\cdot,\cdot))$, is fully specified using a prior mean $\hat{h}:\mathcal{Q}\to\mathbb{R}$ and a positive definite kernel function $k_h:\mathcal{Q}\times\mathcal{Q}\to\mathbb{R}_{>0}$ [1]. The mean function incorporates prior model knowledge, which we set to $\hat{h}(\cdot)=0$ if no prior knowledge about the function is available. This is also assumed in the following without loss of generality. The kernel function $k_h(\cdot,\cdot)$ encodes abstract information about the structure of $h(\cdot)$, such as smoothness or periodicity. In the subsequent sections, we assume that the kernel satisfies the following properties.

Assumption 5: The kernel $k_h(\cdot,\cdot)$ is stationary, i.e., it is a function of the difference of its arguments, and satisfies $k_h(\boldsymbol{q},\boldsymbol{q})=s_h^2$ for all $\boldsymbol{q}\in\mathcal{Q}$, where $s_h^2\in\mathbb{R}_{\geq 0}$ denotes the signal variance.

The stationarity holds for many commonly used kernels, such as the square exponential kernel and Matérn class kernels, which have the capability of approximating continuous functions arbitrarily well [1], [28]. Therefore, this assumption does not impose significant restrictions.

Given training data $\mathbb{D}=\{\boldsymbol{q}^{(i)},y^{(i)}\}_{i=1}^N$ consisting of N training inputs $\boldsymbol{q}^{(i)}\in\mathcal{Q}$ and noisy measurements $y^{(i)}=h(\boldsymbol{q}^{(i)})+\omega^{(i)}$, $\omega^{(i)}\sim\mathcal{N}(0,\sigma_{\text{on}}^2)$, $\sigma_{\text{on}}^2\in\mathbb{R}_{>0}$, we can compute the posterior GP by conditioning the prior on $\mathbb{D}$. The resulting posterior distribution is again Gaussian with mean and variance defined by

$$\mu(\boldsymbol{q})=\boldsymbol{k}_h^T(\boldsymbol{q})\left(\boldsymbol{K}_h+\sigma_{\text{on}}^2\boldsymbol{I}_N\right)^{-1}\boldsymbol{y}, \tag{7a}$$

$$\sigma^2(\boldsymbol{q})=k_h(\boldsymbol{q},\boldsymbol{q})-\boldsymbol{k}_h^T(\boldsymbol{q})\left(\boldsymbol{K}_h+\sigma_{\text{on}}^2\boldsymbol{I}_N\right)^{-1}\boldsymbol{k}_h(\boldsymbol{q}), \tag{7b}$$

where $\boldsymbol{k}_h(\boldsymbol{q})$ and $\boldsymbol{K}_h$ are defined element-wise via $k_{h,i}(\boldsymbol{q})=k_h(\boldsymbol{q},\boldsymbol{q}^{(i)})$ and $K_{h,ij}=k(\boldsymbol{q}^{(i)},\boldsymbol{q}^{(j)})$, respectively, and $\boldsymbol{y}=[y^{(1)}\ \cdots\ y^{(N)}]^T$.

B. Learning Models of Control-Affine Systems

Since in the system (1), the known dynamics is disturbed by the control-affine nonlinearity $f(\boldsymbol{x})+g(\boldsymbol{x})u$, our learned system model should exploit this knowledge and provide a model of the same structure. Including this knowledge of the internal structure of the unknown nonlinearity can be straightforwardly achieved with GPs by employing composite kernels for regression [29]. For this purpose, we define a GP prior for $f(\cdot)$ and $g(\cdot)$ in (1) such that

$$f(\cdot)\sim\mathcal{GP}\left(0,k_f\left(\cdot,\cdot\right)\right), \tag{8a}$$

$$g(\cdot)\sim\mathcal{GP}\left(0,k_g\left(\cdot,\cdot\right)\right) \tag{8b}$$

with $s_f^2=k_f(\boldsymbol{x},\boldsymbol{x})$, $s_g^2=k_g(\boldsymbol{x},\boldsymbol{x})$, where s_f and s_g denote the signal variances of $f(\cdot)$ and $g(\cdot)$, respectively. This implies that the composite prior $h(\cdot)\sim\mathcal{GP}(0,k_h(\cdot,\cdot))$ for $h(\boldsymbol{q})=f(\boldsymbol{x})+g(\boldsymbol{x})u$ with $\boldsymbol{q}=[\boldsymbol{x}^T,u]^T$ is defined via the composite kernel [29],

$$k_h(\boldsymbol{q},\boldsymbol{q})=k_f(\boldsymbol{x},\boldsymbol{x}')+uk_g(\boldsymbol{x},\boldsymbol{x}')u'. \tag{9}$$

Using these priors, it is straightforward to derive the posterior distributions of the functions $f(\cdot)$ and $g(\cdot)$ analogously to standard GPR by conditioning the joint prior of the individual functions on the training data [30]. The resulting posterior distributions are again Gaussian with means and variances

$$\mu_f(\boldsymbol{x}) = \boldsymbol{k}_f^T(\boldsymbol{x})\left(\boldsymbol{K}_h + \sigma_{\text{on}}^2\boldsymbol{I}_N\right)^{-1}\boldsymbol{y}, \tag{10a}$$

$$\mu_g(\boldsymbol{x}) = \boldsymbol{k}_g^T(\boldsymbol{x})\boldsymbol{U}\left(\boldsymbol{K}_h + \sigma_{\text{on}}^2\boldsymbol{I}_N\right)^{-1}\boldsymbol{y}, \tag{10b}$$

$$\sigma_f^2(\boldsymbol{x}) = k_f(\boldsymbol{x},\boldsymbol{x}) - \boldsymbol{k}_f^T(\boldsymbol{x})\left(\boldsymbol{K}_h + \sigma_{\text{on}}^2\boldsymbol{I}_N\right)^{-1}\boldsymbol{k}_f(\boldsymbol{x}), \tag{10c}$$

$$\sigma_g^2(\boldsymbol{x}) = k_g(\boldsymbol{x},\boldsymbol{x}) - \boldsymbol{k}_g^T(\boldsymbol{x})\boldsymbol{U}\left(\boldsymbol{K}_h + \sigma_{\text{on}}^2\boldsymbol{I}_N\right)^{-1}\boldsymbol{U}\boldsymbol{k}_g(\boldsymbol{x}), \tag{10d}$$

where $\boldsymbol{U} = \text{diag}([u^{(1)} \dots u^{(N)}])$ and $\boldsymbol{k}_f(\boldsymbol{x})$, $\boldsymbol{k}_f(\boldsymbol{x})$ are defined analogously to $\boldsymbol{k}_h(\boldsymbol{x})$. In order to exploit the Bayesian foundations of GP regression for the derivation of prediction error bounds, we make the following assumption.

Assumption 6: The unknown functions $f(\cdot)$ and $g(\cdot)$ are samples from prior GPs (8a) and (8b) defined using kernels $k_f(\cdot,\cdot)$ and $k_g(\cdot,\cdot)$, such that (10a)-(10d) are Lipschitz continuous with Lipschitz constants L_{μ_f}, L_{μ_g}, L_{σ_f}, L_{σ_g}.

This assumption of suitable prior distributions is commonly employed when working with Bayesian models, see e.g., [3], [13]. While it effectively limits the admissible class of unknown functions to the sample space of the GP prior, this restriction is often not severe, in particular when working with universal kernels [28]. Moreover, the requirement of Lipschitz continuous mean and standard deviation functions is generally not restrictive. For stationary kernels, it can be straightforwardly achieved using a sufficient differentiability of the kernel [31]. Therefore, Assumption 6 does not pose a significant limitation. Based on this assumption, we introduce next prediction error bounds for $\mu_f(\cdot)$ and $\mu_g(\cdot)$.

Lemma 2: Consider unknown functions $f(\cdot)$ and $g(\cdot)$ satisfying Assumptions 1 and 6. Moreover, assume that $N \in \mathbb{N}$ observations of $\boldsymbol{x}^{(i)}, y^{(i)}$ are available. Then, for every $\delta \in (0,1)$ and any constants $\underline{\sigma}_f, \underline{\sigma}_g \in \mathbb{R}_{>0}$, the prediction error of GP regression is jointly bounded by

$$|\mu_f(\boldsymbol{x}) - f(\boldsymbol{x})| \leq \sqrt{\beta_f}\max\{\sigma_f(\boldsymbol{x}), \underline{\sigma}_f\}, \tag{11a}$$

$$|\mu_g(\boldsymbol{x}) - g(\boldsymbol{x})| \leq \sqrt{\beta_g}\max\{\sigma_g(\boldsymbol{x}), \underline{\sigma}_g\}, \tag{11b}$$

for all $\boldsymbol{x} \in \mathcal{X}$ with probability of at least $1 - \delta$, where

$$\beta_f = 8\log\Big(\frac{2}{\delta}\prod_{j=1}^n\Big(\frac{\sqrt{n}}{2\tau_f}\big(\max_{\boldsymbol{x}\in\mathcal{X}} x_j - \min_{\boldsymbol{x}\in\mathcal{X}} x_j\big) + 1\Big)\Big), \tag{12a}$$

$$\beta_g = 8\log\Big(\frac{2}{\delta}\prod_{j=1}^n\Big(\frac{\sqrt{n}}{2\tau_g}\big(\max_{\boldsymbol{x}\in\mathcal{X}} x_j - \min_{\boldsymbol{x}\in\mathcal{X}} x_j\big) + 1\Big)\Big), \tag{12b}$$

$$\tau_f = \frac{\underline{\sigma}_f}{(L_f + L_{\mu_f} + L_{\sigma_f})}, \tag{12c}$$

$$\tau_g = \{\frac{\underline{\sigma}_g}{(L_g + L_{\mu_g} + L_{\sigma_g})}. \tag{12d}$$

Proof: By slightly adapting [29, Lemma 1], we obtain

$$|\mu_f(\boldsymbol{x}) - f(\boldsymbol{x})| \leq \frac{\sqrt{\beta_f}}{2}\sigma_f(\boldsymbol{x}) + (L_f + L_{\mu_f} + \frac{\sqrt{\beta_f}}{2}L_{\sigma_f})\tau_f \tag{13}$$

for all $\boldsymbol{x} \in \mathcal{X}$ with probability of at least $1 - \delta/2$. Since the right side of this inequality is linear in $\sigma_f(\cdot)$ and $\sigma_f(\boldsymbol{x}) \leq \max\{\sigma_f(\boldsymbol{x}), \underline{\sigma}_f\}$, we substitute $\max\{\sigma_f(\boldsymbol{x}), \underline{\sigma}_f\}$ to obtain

$$|\mu_f(\boldsymbol{x}) - f(\boldsymbol{x})| \leq \frac{\sqrt{\beta_f}}{2}\max\{\sigma_f(\boldsymbol{x}), \underline{\sigma}_f\} + (L_f + L_{\mu_f} + \frac{\sqrt{\beta_f}}{2}L_{\sigma_f})\tau_f. \tag{14}$$

Furthermore, $\max_{\boldsymbol{x}\in\mathbb{X}} x_j - \min_{\boldsymbol{x}\in\mathbb{X}} x_j$ is lower bounded by 0, such that the argument of the logarithm in (12a) is lower bounded by $\frac{2}{\delta}$. As $\delta \in (0,1)$, it follows that $\frac{\beta_f}{4} \geq 2\log(\frac{2}{\delta}) > 1$, such that it holds that

$$(L_f + L_{\mu_f} + \frac{\sqrt{\beta_f}}{2}L_{\sigma_f})\tau_f \leq \frac{\sqrt{\beta_f}}{2}(L_f + L_{\mu_f} + L_{\sigma_f})\tau_f. \tag{15}$$

Using (12c), the right-hand side can be bounded by

$$\frac{\sqrt{\beta_f}}{2}(L_f + L_{\mu_f} + L_{\sigma_f})\tau_f \leq \frac{\sqrt{\beta_f}}{2}\underline{\sigma}_f \tag{16}$$

Finally, noting that $\underline{\sigma}_f \leq \max\{\sigma_f(\boldsymbol{x}), \underline{\sigma}_f\}$, we obtain (11a). The proof for (11b) follows analogously, such that the result is a consequence of the union bound. ■

By exploiting the Bayesian foundation of GPs, this result provides us with probabilistic uniform prediction error bounds for $f(\cdot)$ and $g(\cdot)$ individually. The error bounds in the right-hand side of (11) have only $\underline{\sigma}_f$ and $\underline{\sigma}_g$ as design parameters, which have an intuitive interpretation: they provide a lower bound on the certifiable prediction error. This lower bound can be made arbitrarily small but, according to (12), a reduction of $\underline{\sigma}_f$ and $\underline{\sigma}_g$ is accompanied by an increase of the scaling factors β_f and β_g. One option for choosing the parameters $\underline{\sigma}_f$ and $\underline{\sigma}_g$ is to define $\underline{\sigma}_f = \min_{\boldsymbol{x}\in\mathcal{X}} \sigma_f(\boldsymbol{x})$ and $\underline{\sigma}_g = \min_{\boldsymbol{x}\in\mathcal{X}} \sigma_g(\boldsymbol{x})$ for fixed data sets. When the GP model is learned online, this approach would require the numerical computation of the minima after each model update, which can be computationally prohibitive. An approach to mitigate this issue will be introduced in Section III-D.

C. Safe Learning-Based Control Synthesis

While we assume to not have access to the functions $f(\cdot)$ and $g(\cdot)$, GP regression allows us to infer models in the form of $\mu_f(\cdot)$ and $\mu_g(\cdot)$ from training data. Since these models come along with error bounds, cf. Lemma 2, we robustify the CBF condition (5b) to account for model uncertainty. However, even an infinitesimal increase of the conservatism of (5b) can render this constraint infeasible. For example, if $c(\boldsymbol{x}) = 0$ and $\nabla_{\boldsymbol{x}}^T\psi(\boldsymbol{x}) = 0$ such that $d(\boldsymbol{x}) = 0$, (5b) is feasible, but any perturbation $\epsilon \in \mathbb{R}_{>0}$ renders the condition $c(\boldsymbol{x}) + \epsilon + d(\boldsymbol{x})u \geq 0$ infeasible. Thus, we require an additional assumption on the form of CBF that excludes this scenario, which we specify as follows.

Assumption 7: There exist constants $\zeta_1, \zeta_2 \in \mathbb{R}_{>0}$ such that

$$\alpha(\psi(\boldsymbol{x})) \geq -\nabla_{\boldsymbol{x}}^T\psi(\boldsymbol{x})\boldsymbol{A}\boldsymbol{x} + \zeta_2 \quad \forall \boldsymbol{x}\colon |\nabla_{\boldsymbol{x}}^T\psi(\boldsymbol{x})\boldsymbol{b}| \leq \zeta_1. \tag{17}$$

This assumption essentially requires that the CBF $\psi(\cdot)$ does not have a vanishing gradient in a neighborhood of the boundary of the safe set where $\psi(\boldsymbol{x}) = 0$. If this requirement is satisfied, $\alpha(\cdot)$ can always be chosen such that (17) holds with arbitrarily large value ζ_2. Hence, Assumption 7 is not restrictive in general. The practical implications of Assumption 7 are simple: Whenever the gradient of the CBF $\psi(\boldsymbol{x})$ is small, a sufficiently large value of ζ_2 in (17) ensures that small perturbations cannot change the sign of $c(\boldsymbol{x})$ in (5b). Thereby, this assumption guarantees that sufficiently small learning errors cannot render proofs of safety based on the CBF $\psi(\cdot)$ invalid. Before stating our result on the safe control with GP models, we introduce the shortand notation

$$\tilde{\sigma}_f(\boldsymbol{x}) = \max\{\sigma_f(\boldsymbol{x}), \underline{\sigma}_f\}, \tag{18a}$$

$$\tilde{\sigma}_g(\boldsymbol{x}) = \max\{\sigma_g(\boldsymbol{x}), \underline{\sigma}_g\}. \tag{18b}$$

These functions allow us to formulate the safety filter depicted in Fig. 1 in a compact form and synthesize a safe control law $\pi(\cdot)$ by solving a modified QP. The following result identifies the necessary criteria to ensure safety using learned GP models.

Proposition 1: Consider a system (1), GP priors (8a), (8b) and a fixed data set $\mathbb{D}$ such that Assumptions 1 - 3, 6, and 7 are satisfied with $\zeta_2 = \zeta_1(\bar{f} + 2\sqrt{\beta_f} s_f)$ in (17). Assume that

$$\frac{\mu_g(\boldsymbol{x})}{\sqrt{\beta_g}\tilde{\sigma}_g(\boldsymbol{x})} > 1, \tag{19}$$

holds for all $\boldsymbol{x} \in \mathbb{R}^n$. Then, the control law

$$\pi(\boldsymbol{x}) = \min_u \quad \|u - \pi_{\text{nom}}(\boldsymbol{x})\| \tag{20a}$$

$$\text{s.t. } \xi_s(\boldsymbol{x})u \leq \xi_3(\boldsymbol{x}), \tag{20b}$$

where $\pi_{\text{nom}} : \mathcal{X} \to \mathbb{R}$ is a Lipschitz nominal control law and

$$\xi_s(\boldsymbol{x}) = \text{sgn}(\xi_2(\boldsymbol{x})\xi_3(\boldsymbol{x}))\xi_1(\boldsymbol{x}) + \xi_2(\boldsymbol{x}), \tag{21a}$$

$$\xi_1(\boldsymbol{x}) = \left|\nabla_{\boldsymbol{x}}^T \psi(\boldsymbol{x})\boldsymbol{b}\right| \sqrt{\beta_g}\tilde{\sigma}_g(\boldsymbol{x}), \tag{21b}$$

$$\xi_2(\boldsymbol{x}) = -\nabla_{\boldsymbol{x}}^T \psi(\boldsymbol{x})\boldsymbol{b}\mu_g(\boldsymbol{x}), \tag{21c}$$

$$\begin{aligned}\xi_3(\boldsymbol{x}) = \alpha(\psi(\boldsymbol{x})) + \nabla_{\boldsymbol{x}}^T \psi(\boldsymbol{x})\boldsymbol{A}\boldsymbol{x} + \nabla_{\boldsymbol{x}}^T \psi(\boldsymbol{x})\boldsymbol{b}\mu_f(\boldsymbol{x}) \\ - \left|\nabla_{\boldsymbol{x}}^T \psi(\boldsymbol{x})\boldsymbol{b}\right| \sqrt{\beta_f}\tilde{\sigma}_f(\boldsymbol{x}),\end{aligned} \tag{21d}$$

is feasible and ensures safety for all $t \in \mathbb{R}_{\geq 0}$ with probability of at least $1 - \delta$.

Proof: We approximate the unknown parts $f(\cdot)$ and $g(\cdot)$ of (1) with the GP models $\mu_f(\cdot)$ and $\mu_g(\cdot)$ to obtain

$$\dot{\boldsymbol{x}} = \boldsymbol{A}\boldsymbol{x} + \boldsymbol{b}(e_f(\boldsymbol{x}) + \mu_f(\boldsymbol{x}) + (e_g(\boldsymbol{x}) + \mu_g(\boldsymbol{x}))u), \tag{22}$$

where

$$e_f(\boldsymbol{x}) = f(\boldsymbol{x}) - \mu_f(\boldsymbol{x}),$$
$$e_g(\boldsymbol{x}) = g(\boldsymbol{x}) - \mu_g(\boldsymbol{x}),$$

denote the errors between the real and learned models. Substituting (22) in the CBF constraint (5b), we obtain

$$\begin{aligned}\nabla_{\boldsymbol{x}}^T \psi(\boldsymbol{x})\big(\boldsymbol{A}\boldsymbol{x} + \boldsymbol{b}\big(e_f(\boldsymbol{x}) + \mu_f(\boldsymbol{x}) + \big(e_g(\boldsymbol{x}) + \mu_g(\boldsymbol{x})\big)u\big)\big) \\ \geq -\alpha(\psi(\boldsymbol{x})).\end{aligned} \tag{23}$$

Note that we cannot directly enforce constraint (23) via the learned dynamics, as it relies on the unknown model errors $e_f(\cdot)$ and $e_g(\cdot)$. Instead, we derive a probabilistic worst-case evaluation of (23) by employing Lemma 2 to obtain

$$\begin{aligned}\left\|\nabla_{\boldsymbol{x}}^T \psi(\boldsymbol{x})\boldsymbol{b}\right\| \sqrt{\beta_g}\tilde{\sigma}_g(\boldsymbol{x})|u| - \nabla_{\boldsymbol{x}}^T \psi(\boldsymbol{x})\boldsymbol{b}\mu_g(\boldsymbol{x})u \leq \alpha(\psi(\boldsymbol{x})) + \\ \nabla_{\boldsymbol{x}}^T \psi(\boldsymbol{x})\boldsymbol{A}\boldsymbol{x} + \nabla_{\boldsymbol{x}}^T \psi(\boldsymbol{x})\boldsymbol{b}\mu_f(\boldsymbol{x}) - \left\|\nabla_{\boldsymbol{x}}^T \psi(\boldsymbol{x})\boldsymbol{b}\right\|\sqrt{\beta_f}\tilde{\sigma}_f(\boldsymbol{x}),\end{aligned} \tag{24}$$

which holds with probability of at least $1 - \delta$. Using the definition of $\xi_i(\cdot)$ in (21b)-(21d), we can compactly express this as

$$\xi_1(\boldsymbol{x})|u| + \xi_2(\boldsymbol{x})u \leq \xi_3(\boldsymbol{x}). \tag{25}$$

For all states $\boldsymbol{x} \in \mathcal{C}$ which satisfy $|\nabla_{\boldsymbol{x}}^T \psi(\boldsymbol{x})\boldsymbol{b}| > 0$, we immediately obtain $\xi_1(\boldsymbol{x}) > 0$. Moreover, it follows from (19) that $\xi_1(\boldsymbol{x}) < |\xi_2(\boldsymbol{x})|$. From Lemma 3 in the Appendix, we can equivalently express (25) as (20b). This allows us to solve the optimization problem (20) analytically, such that it is straightforward to show that

$$\pi(\boldsymbol{x}) = \begin{cases} \pi_{\text{nom}}(\boldsymbol{x}), & \text{if } \xi_s(\boldsymbol{x})\pi_{\text{nom}}(\boldsymbol{x}) \leq \xi_3(\boldsymbol{x}) \\ \frac{\xi_3(\boldsymbol{x})}{\xi_s(\boldsymbol{x})}, & \text{else.} \end{cases} \tag{26}$$

Moreover, due to the definition of $\xi_s(\cdot)$ in (21a), this control law can be equivalently expressed as

$$\pi(\boldsymbol{x}) = \begin{cases} \pi_{\text{nom}}(\boldsymbol{x}), & \text{if } \xi_s(\boldsymbol{x})\pi_{\text{nom}}(\boldsymbol{x}) \leq \xi_3(\boldsymbol{x}) \\ \frac{\xi_3(\boldsymbol{x})}{\xi_2(\boldsymbol{x})+\xi_1(\boldsymbol{x})}, & \text{else if } \xi_2(\boldsymbol{x})\xi_3(\boldsymbol{x}) > 0 \\ \frac{\xi_3(\boldsymbol{x})}{\xi_2(\boldsymbol{x})-\xi_1(\boldsymbol{x})}, & \text{else.} \end{cases} \tag{27}$$

When $|\nabla_{\boldsymbol{x}}^T \psi(\boldsymbol{x})\boldsymbol{b}| = 0$, Lemma 3 is inapplicable since $\xi_1(\boldsymbol{x}) = \xi_2(\boldsymbol{x}) = 0$. However, Assumption 7 with $\zeta_2 = \zeta_1(\bar{f} + 2\sqrt{\beta_f} s_f)$ guarantees that $\xi_3(\boldsymbol{x}) \geq 0$ since

$$\begin{aligned}\nabla_{\boldsymbol{x}}^T \psi(\boldsymbol{x})\boldsymbol{b}\mu_f(\boldsymbol{x}) \geq -\zeta_1(\bar{f} + \sqrt{\beta_f} s_f) \\ - \left|\nabla_{\boldsymbol{x}}^T \psi(\boldsymbol{x})\boldsymbol{b}\right| \sqrt{\beta_f}\tilde{\sigma}_f(\boldsymbol{x}) \geq -\zeta_1\sqrt{\beta_f} s_f\end{aligned}$$

with probability $1 - \delta$ for all $\boldsymbol{x}$ with $|\nabla_{\boldsymbol{x}}^T \psi(\boldsymbol{x})\boldsymbol{b}| \leq \zeta_1$. Thus, it follows that every control input u satisfies (25) when $|\nabla_{\boldsymbol{x}}^T \psi(\boldsymbol{x})\boldsymbol{b}| = 0$, which implies that the optimal control input is given by $\pi_{\text{nom}}(\boldsymbol{x})$. Since $|\nabla_{\boldsymbol{x}}^T \psi(\boldsymbol{x})\boldsymbol{b}| = 0$ implies $\xi_s(\boldsymbol{x}) = 0$, this is also the control input provided by (27), such that this control law can be applied without a separate distinction based on $|\nabla_{\boldsymbol{x}}^T \psi(\boldsymbol{x})\boldsymbol{b}|$. Hence, the control law (20) is feasible. Note that the switching between $\pi_{\text{nom}}(\cdot)$ and $\xi_3(\boldsymbol{x})/\xi_s(\boldsymbol{x})$ in (27) is continuous as

$$\pi_{\text{nom}}(\boldsymbol{x}) = \frac{\xi_3(\boldsymbol{x})}{\xi_s(\boldsymbol{x})} \qquad \forall \boldsymbol{x} : \xi_s(\boldsymbol{x})\pi_{\text{nom}}(\boldsymbol{x}) = \xi_3(\boldsymbol{x}). \tag{28}$$

When $\xi_3(\boldsymbol{x}) = 0$, the switching in (27) is also continuous due to

$$\frac{\xi_3(\boldsymbol{x})}{\xi_2(\boldsymbol{x}) + \xi_1(\boldsymbol{x})} = \frac{\xi_3(\boldsymbol{x})}{\xi_2(\boldsymbol{x}) - \xi_1(\boldsymbol{x})} = 0. \tag{29}$$

Finally, $\xi_2(\boldsymbol{x}) = 0$ implies $\nabla_{\boldsymbol{x}}^T \psi \boldsymbol{b} = 0$ due to (19), such that Assumption 7 guarantees $\pi(\boldsymbol{x}) = \pi_{\text{nom}}(\boldsymbol{x})$ as shown before. Hence, the control law cannot switch from $\xi_3(\boldsymbol{x})/(\xi_2(\boldsymbol{x})+\xi_1(\boldsymbol{x}))$ to $\xi_3(\boldsymbol{x})/(\xi_2(\boldsymbol{x})-\xi_1(\boldsymbol{x}))$ when $\xi_2(\boldsymbol{x}) = 0$. Since all of the control laws in (27) are Lipschitz continuous on $\mathbb{R}^n$ due to the assumed smoothness properties of $\pi_{\text{nom}}(\cdot)$, $\psi(\cdot)$, $\alpha(\cdot)$, $\mu_f(\cdot)$, $\mu_g(\cdot)$, $\sigma_f(\cdot)$, and $\sigma_g(\cdot)$, and the switching between them is continuous, it can be straightforwardly seen that, given points $\boldsymbol{x}, \boldsymbol{x}'$ such that $\xi_s(\boldsymbol{x})\pi_{\text{nom}}(x) \leq \xi_3(\boldsymbol{x})$ and $\xi_s(\boldsymbol{x}')\pi_{\text{nom}}(\boldsymbol{x}') > \xi_3(\boldsymbol{x}')$, we obtain

$$\begin{aligned}|\pi(\boldsymbol{x}) - \pi(\boldsymbol{x}')| &\leq L_1 |\boldsymbol{x} - \boldsymbol{x}_{\boldsymbol{s}}| + L_{2,3} |\boldsymbol{x}_{\boldsymbol{s}} - \boldsymbol{x}'| \\ &\leq \max\{L_1, L_{2,3}\}\|\boldsymbol{x} - \boldsymbol{x}'\|,\end{aligned}$$

where $L_1, L_{2,3} \in \mathbb{R}_{>0}$ are Lipschitz constants of the first and second/third line of (27) and $\boldsymbol{x}_s \in \mathbb{R}^n$ is the point on the straight line connecting $\boldsymbol{x}$, $\boldsymbol{x}'$ with $\xi_s(\boldsymbol{x}')\pi_{\mathrm{nom}}(\boldsymbol{x}') = \xi_3(\boldsymbol{x}')$. Therefore, $\pi(\cdot)$ is globally Lipschitz continuous, such that the right-hand side of (1) with $u = \pi(\boldsymbol{x})$ is globally Lipschitz continuous and consequently, existence and uniqueness of the solution of (1) under the control law (20) are guaranteed for all $t \in \mathbb{R}_{\geq 0}$ [21, Theorem 3.1]. Forward invariance with probability of at least $1-\delta$ immediately follows from Nagumo's theorem [32, Theorem 4.7] because the CBF constraint (5b) is satisfied by construction since (23) reflects its probabilistic worst case. Thus, the controlled system is safe with probability $1-\delta$, which concludes the proof. ■

Proposition 1 allows us the straightforward design of a safe control law, even though we only have access to the learned models $\mu_f(\cdot)$ and $\mu_g(\cdot)$. For achieving this, we merely need to check condition (19), which essentially requires a sufficiently small posterior standard deviation $\sigma_g(\boldsymbol{x})$ for all $\boldsymbol{x} \in \mathcal{C}$ together with a sufficiently small value $\underline{\sigma}_g$. The reason for this requirement can intuitively be explained as follows. Due to the decoupling into the nominal behavior defined through $\mu_g(\cdot)$ and the learning error $e_g(\cdot)$ in (22), we need to ensure that the error term $e_g(\boldsymbol{x})u$ cannot dominate the nominal effect $\mu_g(\boldsymbol{x})u$ of the control input u. This can be excluded if

$$\mu_g(\boldsymbol{x}) > e_g(\boldsymbol{x}). \tag{30}$$

While a direct evaluation of this inequality is not feasible due to the limited knowledge of $g(\cdot)$, we can leverage the prediction error bound for GPs of Lemma 2 to address this. Therefore, we obtain (19) as a sufficient condition with probability $1-\delta$. This condition can consequently be interpreted as an excitation condition ensuring the sufficiently accurate identification of the GP model.

The implications of (19) are significant: it allows us to handle the absolute value $|u|$ in (24) using Lemma 3. This enables us to show that the resulting control (20) is Lipschitz continuous. This is in contrast to [18], where only local Lipschitz continuity of the policy is shown, which restricts the guaranteed existence of a solution to (1) under their controller to finite time intervals. Note that the usage of Lemma 3 also has practical implications: Proposition 1 allows us to solve a QP (20), whereas SOCP are required in all other existing combinations of GPs with CBFs to the best of our knowledge. Therefore, Proposition 1 generally admits a computationally more efficient implementation.

Remark 3: Proposition 1 extends to systems with multiple inputs for which positive definitess of individual elements of the matrix $\boldsymbol{G}(\boldsymbol{x})$ guarantees the positive definiteness (and thus invertibility) of $\boldsymbol{G}(\boldsymbol{x})$. Therefore, the extension to multi-input systems characterized by a block-diagonal matrix $\boldsymbol{B} \in \mathbb{R}^{n\times n}$ and a diagonal matrix $\boldsymbol{G}(\boldsymbol{x}) \in \mathbb{R}^{n\times n}$, as mentioned in Remark 1, can be achieved by employing multiple GP models, each of them inducing an individual excitation condition of the form (19). Note that the extension to a wider class of control-affine systems can be achieved by deriving a vector-valued analog to Lemma 3, which is left for future work.

D. Event-Triggered Learning for Feasibility Guarantees

While Proposition 1 provides a straightforward and computationally efficient approach for ensuring safety using learned GP models, it requires that (19) is satisfied for all $\boldsymbol{x} \in \mathcal{X}$. This assumption can be challenging to ensure and formally showing that it holds requires determining the global minimum of the left-hand side of (19), which is a non-convex function in general. Thus, an intuitive approach is to update the GP model online to improve its accuracy, thereby maintaining the satisfaction of (19) if it holds at an initial state. However, arbitrary training data does not achieve this goal in general. Consider for example the scenario where for the system (1), a training sample $([\boldsymbol{x}^T, u]^T, y)$ with zero control input is added to an existing data set to update the GP model. Then, one sees from (10b) and (10d) that $\mu_g(\cdot)$ and $\sigma_g(\cdot)$ are not affected by the update. This is intuitive as it is simply not possible to extract any information about $g(\cdot)$ from this additional data. This example motivates the need for a control law that provides a sufficient excitation during data collection phases such that uncertainty about $g(\cdot)$ can be effectively reduced. As we can only maintain safety when (19) is satisfied, the goal of this control law is the generation of data that increases $\mu_g(\boldsymbol{x})/\sqrt{\beta_g}\tilde{\sigma}_g(\boldsymbol{x})$ whenever it approaches 1, such that (19) continues to be satisfied for after the update. Such a control law can be obtained by modifying the design (20) using an excitation filter as shown in Fig. 1, which is stated in the following result.

Proposition 2: Consider a system (1), GP priors (8a), (8b) and a fixed data set $\mathbb{D}$ such that Assumptions 1 - 7 are satisfied with $\zeta_2 = \zeta_1(\bar{f} + 2\sqrt{\beta_f}s_f)$ in (17). Moreover, choose $\underline{\sigma}_g \in \mathbb{R}_{>0}$ such that

$$\sqrt{\beta_g}\underline{\sigma}_g \leq \frac{\underline{g}}{1+\epsilon+\gamma} \tag{31}$$

for some constants $\epsilon, \gamma \in \mathbb{R}_{>0}$ and assume that $s_g^2 = k_g(\boldsymbol{x},\boldsymbol{x}) > \underline{\sigma}_g^2$. If (19) holds at a state $\boldsymbol{x} \in \mathbb{R}^n$, then with probability of at least $1-\delta$, the control input $u = \bar{\pi}(\boldsymbol{x})$ is well-defined and satisfies (20b), where

$$\bar{\pi}(\boldsymbol{x}) = \begin{cases} \pi(\boldsymbol{x}) & \text{if } |\pi(\boldsymbol{x})| \geq \underline{u}_{\mathrm{GP}} \\ -\mathrm{sgn}(\xi_s(\boldsymbol{x}))\underline{u}_{\mathrm{GP}} & \text{else,} \end{cases} \tag{32}$$

$\pi(\cdot)$ is defined in (20) and the constant $\underline{u}_{GP}$ is defined through

$$\underline{u}_{GP} = \sqrt{\frac{((1+\epsilon+\gamma)^2\beta_g s_g^2 - \underline{g}^2)(s_f^2 + s_{\mathrm{on}}^2)}{\underline{g}^2}}. \tag{33}$$

Moreover, the GP model trained with an updated data set $\mathbb{D} \cup \{[\boldsymbol{x}, \bar{\pi}(\boldsymbol{x})]^T, y\}$ guarantees that

$$\frac{\mu_g(\boldsymbol{x})}{\sqrt{\beta_g}\sigma_g(\boldsymbol{x})} \geq 1+\epsilon+\gamma. \tag{34}$$

Proof: Since (19) holds, (20) is well-defined and ensures the satisfaction of (5b), i.e., it is safe. Furthermore, (20) satisfies $\xi_s(\boldsymbol{x})\pi(\boldsymbol{x}) \leq \xi_3$ by construction and consequently, it follows from the proof of Proposition 1 that the satisfaction of (5b) is also ensured through the constraint

$$\mathrm{sgn}(\xi_s(\boldsymbol{x}))u \leq \mathrm{sgn}(\xi_s(\boldsymbol{x}))\pi(\boldsymbol{x}). \tag{35}$$

Thus, it can be straightforwardly seen that the filter (32) only modifies $\pi(\cdot)$ in a safe direction when $|\pi(\boldsymbol{x})| \geq \underline{u}_{\mathrm{GP}}$, such that $\bar{\pi}(\boldsymbol{x})$ also satisfies (5b). It remains to show that (34) holds. Assume $\sigma_g(\boldsymbol{x}) \leq \underline{\sigma}_g$. Then, we have

$$\begin{aligned}\frac{\mu_g(\boldsymbol{x})}{\sqrt{\beta_g}\max\{\sigma_g(\boldsymbol{x}),\underline{\sigma}_g\}} &\geq \frac{\underline{g}-\sqrt{\beta_g}\underline{\sigma}_g}{\sqrt{\beta_g}\underline{\sigma}_g}\\ &\geq 1+\epsilon+\gamma, \end{aligned} \tag{36}$$

where the second line follows from (31). We can completely focus on the case $\sigma_g(\boldsymbol{x}) > \underline{\sigma}_g$ and solve (34) for $\sigma_g(\boldsymbol{x})$ using the same inequalities as in (36), which yields the condition

$$\sigma_g^2(\boldsymbol{x}) \leq \frac{\underline{g}^2}{(1+\epsilon+\gamma)^2\beta_g}. \tag{37}$$

Due to [29, Theorem 1], this can be enforced through the requirement

$$s_g^2 - \frac{s_g^4\bar{\pi}^2(\boldsymbol{x})}{s_f^2+\bar{\pi}^2(\boldsymbol{x})s_g^2+\sigma_{\mathrm{on}}^2} \leq \frac{\underline{g}^2}{(1+\epsilon+\gamma)^2\beta_g} \tag{38}$$

on the new data pair $([\boldsymbol{x}^T,\bar{\pi}(\boldsymbol{x})]^T, y)$. Solving this inequality for $|\bar{\pi}(\boldsymbol{x})|$ results in $|\bar{\pi}(\boldsymbol{x})| \geq \underline{u}_{GP}$, where $\underline{u}_{GP}$ is defined via (33), such that the updated GP will satisfy (34) by construction. ■

Since Proposition 2 modifies the control inputs based on (20), most assumptions are identical to the ones in Proposition 1. However, it requires a tightened condition for $\underline{\sigma}_g$ in order to allow to sufficiently reduce $\tilde{\sigma}(\cdot)$ through additional training data. This effectively renders the lower bound $\underline{\sigma}_g$ irrelevant for the analysis in the proof of Proposition 2. Based on this property, the excitation filter (32) essentially restricts the control input to sufficiently high amplitudes, but modifies it in a safe direction. Our approach does not just specify the direction in which the control input needs to be adapted, but it directly provides its value through $\underline{u}_{GP}$. This value can easily be computed and depends on the design parameters ϵ and γ as well as hyperparameters s_g, s_f and s_{on}. Moreover, it provides a useful intuition about the need for excitation: when

$$s_g < \frac{\underline{g}}{(1+\epsilon+\gamma)\sqrt{\beta_g}} \tag{39}$$

holds, i.e., the prior GP error bound for $g(\cdot)$ already satisfies (19), the lower bound $\underline{u}_{GP}$ becomes complex valued. Therefore, (32) and (20) become identical, such that no additional excitation is enforced by (32). Since the whole motivation behind this control law is to ensure the satisfaction of (19) which is already guaranteed through the prior, this fall-back to the safety-filtered control law $\pi(\cdot)$ is a natural behavior.

When s_g is not small enough to ensure (39), the amplitude of the excitation filtered controller $\bar{\pi}(\cdot)$ is larger than that of $\pi(\cdot)$, such that the difference to the nominal policy gets increased for (32). Since this generally results in a worse closed-loop performance, it is desirable to use $\bar{\pi}(\cdot)$ only when we collect training samples. Therefore, we distinguish two phases with different goals in our overall control approach:

- When we are at risk of violating (19), we focus on improving the model accuracy and employ the excitation filter (32) to generate informative training samples. We determine the necessity of GP model updates through an event trigger. Given $N \in \mathbb{N}$,

$$t_{N+1} = \inf_{t>t_N} t \tag{40a}$$

$$\text{such that } \frac{\mu_g(\boldsymbol{x}(t))}{\sqrt{\beta_g}\sigma_g(\boldsymbol{x}(t))} \leq 1+\epsilon, \tag{40b}$$

  which is used to activate the excitation filter (32), i.e.,

$$u(t) = \bar{\pi}(\boldsymbol{x}(t)), \qquad t = t_N. \tag{41}$$

  Therefore, new training samples have the form $([\boldsymbol{x}^T(t_{N+1}), \bar{\pi}(\boldsymbol{x}^T(t_{N+1}))]^T, y)$.
- When the model accuracy is sufficient, i.e., (40b) is not satisfied, we focus on control performance and directly apply the safe policy (20) which minimizes the deviation from the nominal control law $\pi_{\mathrm{nom}}(\cdot)$. Thus, we choose the control signal in this phase as

$$u(t) = \pi(\boldsymbol{x}(t)), \qquad \forall t \in (t_N, t_{N+1}), N \in \mathbb{N}. \tag{42}$$

Algorithm 1 Safe Control via Event-Triggered Learning

$N \leftarrow 0$
compute β_f using (12a)
determine β_g, $\underline{\sigma}_g$ by solving (31) and $\underline{u}_{\mathrm{GP}}$ based on (33)
while true do
  compute safety-filtered control $\pi(\boldsymbol{x})$ using (20)
  if $\mu_g(\boldsymbol{x}(t))/\sqrt{\beta_g}\sigma_g(\boldsymbol{x}(t)) = 1+\epsilon$ **then**
    $N \leftarrow N+1$, $t_N = t$
    compute excitation-filtered control $\bar{\pi}(\boldsymbol{x})$ using (32)
    apply $u = \bar{\pi}(\boldsymbol{x})$
    measure $y = f(\boldsymbol{x}(t_N) + g(\boldsymbol{x}(t_N))u + \omega$
    $\mathbb{D} \leftarrow \mathbb{D} \cup \{([\boldsymbol{x}^T(t_N), u]^T, y\}$
    update $\mu_f(\cdot)$, $\mu_g(\cdot)$, $\sigma_f(\cdot)$, $\sigma_g(\cdot)$
  else
    apply $u = \pi(\boldsymbol{x})$
  end if
end while

This event-triggered approach for simultaneous learning and controlling system (1), which is summarized in Algorithm 1, guarantees safety, as shown in the following result.

Theorem 1: Consider a system (1), GP priors (8a), (8b), and a Lipschitz continuous nominal control law $\pi_{\mathrm{nom}}(\cdot)$ such that Assumptions 1 - 7 are satisfied with $\zeta_2 = \zeta_1(\bar{f} + 2\sqrt{\beta_f}s_f)$ in (17). Moreover, assume that $s_g > \underline{\sigma}_g$. Then, for all $N \in \mathbb{N}$, Algorithm 1 with design parameters $\epsilon, \gamma \in \mathbb{R}_{>0}$ yields a well-defined control law and guarantees safety during the time interval $[t_N, t_{N+1})$ with probability of at least $1-\delta$ if (19) and $x(t) \in \mathcal{C}$ are satisfied at $t = t_N$.

Proof: Due to the GP model update event and the satisfaction of (19) at $t = t_N$, Proposition 2 guarantees that (19) holds for all $t \in [t_N, t_{N+1})$, where t_{N+1} is the next trigger time instance defined in (40b). Note that the switching between $\bar{\pi}(\cdot)$ and $\pi(\cdot)$ at $t = t_N$ renders the control law defined through Algorithm 1 discontinuous and a function of the time t. Nevertheless, an extended solution of (1) exists [33, Chapter 2, Theorem 1.1] and is unique [33, Chapter 2, Theorem 2.2] as the right-hand side of (1) under the control law defined by Algorithm 1 is a measurable function in time t, uniformly Lipschitz continuous in $\boldsymbol{x}$, and bounded on the compact set $\mathcal{C}$ due to the Lipschitz continuity of $f(\cdot)$, $g(\cdot)$, $\pi(\cdot)$ and boundedness of $\bar{\pi}(\cdot)$. Since $\boldsymbol{x}(t_N) \in \mathcal{C}$ and (20b) is satisfied with probability of at least $1-\delta$ for all $\boldsymbol{x} \in \mathcal{C}$ and $t \in [t_N, t_{N+1})$ due to Propositions 1 and 2, we employ Nagumo's theorem [32, Theorem 4.7] guaranteeing the forward invariance. Thus, safety is guaranteed during each time interval $[t_N, t_{N+1})$ with probability $1-\delta$. ■

This result guarantees that the system stays in the safe set during the time between two GP update events with probability $1-\delta$ if it starts inside it at a point where (19) is satisfied. This condition is necessary to prevent any safety violations from the control before any safe learning is possible. This is easily satisfied at the initial condition $\boldsymbol{x}(0)$ by initializing the GP model with a suitable prior or by providing training data obtained a priori, e.g., by running a locally safe controller.

It is important to note that the safety guarantee only holds for a single time interval with probability $1-\delta$ since each model update induces a new GP model and requires a new error bound [2], [3]. However, this does not pose a critical limitation since it straightforwardly follows from Theorem 1 and the union bound that for any time interval $[0, t_N]$ safety and feasibility are guaranteed with probability $\max\{0, 1-N\delta\}$. Therefore, choosing a sufficiently small δ can ensure safety for any finite number of sampling events. Since we will show in Proposition 3 that the inter-event time is lower bounded by a positive value, this immediately implies that safety can be guaranteed over arbitrary, finite time intervals $[0, t]$, which illustrates the practical strengths of Theorem 1.

Remark 4: It is possible to extend the safety guarantees to unbounded time intervals $[0, \infty)$ by employing a decaying sequence of δ_N, similarly as proposed in [2], [3], e.g., $\delta_N = \frac{6\delta}{N\pi^2}$, such that $\sum_{N=1}^{\infty} \delta_N = \delta$. However, this leads to a growing scaling factor β_g due to its dependency on δ.

Remark 5: Since the accuracy of our model for $g(\cdot)$ based on condition (19) is crucial for ensuring safety, our proposed event-triggered online learning strategy focuses purely on reducing the uncertainty about $g(\cdot)$. However, this does not mean that the model accuracy for $f(\cdot)$ is irrelevant for the CBF constraints. Since the model error of $\mu_f(\cdot)$ is considered in (21d), high uncertainty about $f(\cdot)$ generally causes more restrictive CBF constraints (20b) and thus higher control effort. Therefore, it is generally beneficial for control performance to also improve the model accuracy of $\mu_f(\cdot)$. This could potentially be achieved by employing an additional event trigger for learning $f(\cdot)$, but the design and detailed analysis of such a trigger are beyond the scope of this paper.

E. Ruling out Zeno Behavior

Avoiding Zeno behavior is crucial in event-triggered learning with GPs to prevent updates from accumulating in a finite amount of time, which would make a practical implementation impossible. In order to exclude Zeno behavior in event-triggered learning, it is sufficient to uniformly lower bound the time between any two consecutive events by a positive constant. This approach is employed in the following result.

Proposition 3: Consider a system (1), and GP priors (8a), (8b) such that Assumptions 1 - 7 are satisfied. Moreover, assume that (19) is satisfied at $t=0$ and $s_g > \underline{\sigma}_g$. Then, with probability of at least $1-\delta$, Algorithm 1 with design parameters $\epsilon, \gamma \in \mathbb{R}_{>0}$ triggers model updates with an inter-event time $\Delta_N = t_{N+1} - t_N$ satisfying $\Delta_N \geq \gamma/L_\Gamma$ for all $N \in \mathbb{N}$, where L_Γ denotes the Lipschitz constant of the triggering function

$$\Gamma(t) = \frac{\mu_g(\boldsymbol{x}(t))}{\sqrt{\beta_g}\tilde{\sigma}_g(\boldsymbol{x}(t))}. \tag{43}$$

Proof: The triggering function $\Gamma(t)$ is Lipschitz continuous because the standard deviation and mean functions are Lipschitz continuous, and $\tilde{\sigma}_g(x)$ is positive. Moreover, the trajectory $\boldsymbol{x}(t)$ is Lipschitz continuous with respect to time since it is the solution of a differential equation defined through bounded closed-loop dynamics, as discussed in the proof of Theorem 1. Let L_Γ denote the Lipschitz constant of $\Gamma(\cdot)$ and let t_N, t_{N+1} denote two consecutive triggering times. Then, we have

$$|\Gamma(t_{N+1}) - \Gamma(t_N)| \leq L_\Gamma(t_{N+1} - t_N). \tag{44}$$

Using the triangle inequality and the positivity of $\Gamma(\cdot)$,

$$\Gamma(t_{N+1}) \geq \Gamma(t_N) - |\Gamma(t_{N+1}) - \Gamma(t_N)|. \tag{45}$$

Therefore, it follows from Proposition 2 that

$$\Gamma(t_{N+1}) \geq 1 + \epsilon + \gamma - L_\Gamma(t_{N+1} - t_N) \tag{46}$$

since t_N is a triggering time at which a model update occurs. Due to the triggering condition (34), we know that the next event occurs when $\Gamma(t_{N+1}) = 1 + \epsilon$. This implies that

$$1 + \epsilon \geq 1 + \epsilon + \gamma - L_\Gamma(t_{N+1} - t_N) \tag{47}$$

must hold. Therefore, we obtain

$$(t_{N+1} - t_N) \geq \Delta_N = \frac{\gamma}{L_\Gamma}, \tag{48}$$

which concludes the proof. ■

This result exploits the Lipschitzness of the state trajectory together with the GP mean $\mu_g(\cdot)$ and the standard deviation $\sigma_g(\cdot)$ to obtain a Lipschitz constant L_Γ. Since update events are triggered with a higher threshold than ensured after the update, the Lipschitz continuity of $\Gamma(\cdot)$ directly implies a lower bound on the inter-event times. The constant L_Γ captures the change rate of the system and the dependency on the GP prior. Intuitively, when the system or the GP model exhibit a high variability, L_Γ is large, so that a high triggering frequency can occur. This can be partially compensated by reducing the gap between the trigger condition and the update objective, which is given by the constant γ. Hence, this parameter allows us to effectively tune the inter-event times of Algorithm 1.

IV. Safe Control Through Event-Triggered Learning for Sampled-Data Systems

To address the challenges faced in practical control applications, we extend the results developed above to sampled-data systems. For this purpose, we introduce the concept of robust sampled-data control barrier functions, which consider model errors and the effects of delays due to sampling in Section IV-A. The safe online learning mechanism for sampled-data systems is presented in Section IV-B.

A. Control Synthesis for Sampled-Data Systems

While the CBF condition (24) is used for ensuring safety using learned GP models, it relies on the assumption that the computed control input is applied continuously. In real-world scenarios, controllers operate in discrete time using fixed sampling frequencies on systems that evolve continuously, therefore, the system must consider the sampled-data control constraint (6). As a result, it becomes necessary to modify the condition (24) to enable the construction of a control law that ensures safety throughout the entire sampling period and prevents safety violations. We address the additional constraint (6) by employing a robust sampled-data version of the CBF constraint (20b) in an input-constrained QP

$$u_k = \min_u \quad \|u - \pi_{\mathrm{nom}}(\boldsymbol{x}_k)\| \tag{49a}$$
$$\tilde{\xi}_s(\boldsymbol{x}_k)u \leq \tilde{\xi}_3(\boldsymbol{x}_k), \tag{49b}$$
$$-\bar{u} \leq u \leq \bar{u} \tag{49c}$$

with

$$\tilde{\xi}_3(\boldsymbol{x}_k) = \xi_3(\boldsymbol{x}_k) - \phi T,$$
$$\tilde{\xi}_s(\boldsymbol{x}_k) = \mathrm{sgn}(\xi_2(\boldsymbol{x}_k)\tilde{\xi}_3(\boldsymbol{x}_k))\xi_1(\boldsymbol{x}_k) + \xi_2(\boldsymbol{x}_k),$$

robustness margin $\phi \in \mathbb{R}_+$, sampled state $\boldsymbol{x}_k = \boldsymbol{x}(kT)$, and control input constraint $\bar{u} \in \mathbb{R}_{>0}$ to obtain a safe control signal $u(t) = u_k$ for all $t \in [kT, (k+1)T)$. The additional input constraint (49c) is essential for deriving a sufficiently large robustness margin ϕ to compensate for effects of the sampled-data realization as we show in the following result.

Proposition 4: Consider a system (1) with sampled-data control constraint (6), GP priors (8a), (8b) and a fixed data set $\mathbb{D}$, and a CBF $\psi(\cdot)$ inducing a bounded safe set $\mathcal{C}$ such that Assumptions 1 - 4, 6, and 7 are satisfied with $\zeta_2 = \zeta_1(\bar{f} + 2\sqrt{\beta_f}s_f) + \tilde{\phi}$, $\tilde{\phi} \in \mathbb{R}_{>0}$, in (17). Assume that

$$\frac{\mu(\boldsymbol{x})}{\sqrt{\beta_g}\tilde{\sigma}_g(\boldsymbol{x})} \geq 1 + \epsilon \tag{50}$$

for all $\boldsymbol{x} \in \mathbb{R}^n$ and some $\epsilon \in \mathbb{R}_{>0}$. If

$$T \leq \max\left\{\frac{\tilde{\phi}}{\phi}, \frac{\zeta_1\epsilon\sqrt{\beta_g}\underline{\sigma}_g\bar{u} - \max_{\boldsymbol{x}\in\mathcal{C}}\xi_3(\boldsymbol{x})}{\phi}\right\}, \tag{51}$$

$$\bar{u} > \frac{\max\limits_{\boldsymbol{x}\in\mathcal{C}}\xi_3(\boldsymbol{x})}{\zeta_1\epsilon\sqrt{\beta_g}\underline{\sigma}_g}, \tag{52}$$

where

$$\phi = ((L_{\xi_1} + L_{\xi_2})\bar{u} + L_{\xi_3})(\bar{f} + \bar{g}\bar{u}) \tag{53}$$

and L_{ξ_i} denote the Lipschitz constants of the functions $\xi_i(\cdot)$, then, the sampled-data controller (49) with robustness margin (53) is feasible and ensures safety for all $t \in \mathbb{R}_{\geq 0}$ with probability of at least $1 - \delta$.

Proof: We prove the result by bounding the difference between the CBF condition (25) evaluated at the sampling times $t_k = kT$ and arbitrary times within the sampling intervals $[t_k, t_k + T)$. For this, we exploit the continuity of the functions $\xi_i(\cdot)$ and the trajectory $\boldsymbol{x}(t)$. Due to the Cauchy-Schwarz inequality and reverse triangle inequality, we have

$$\|\xi_1(\boldsymbol{x}) - \xi_1(\boldsymbol{x_k})\| \leq \|\boldsymbol{b}\|\sqrt{\beta_g}\left\|\nabla_{\boldsymbol{x}}^T\psi(\boldsymbol{x})\tilde{\sigma}_g(\boldsymbol{x}) - \nabla_{\boldsymbol{x}_k}^T\psi(\boldsymbol{x}_k)\tilde{\sigma}_g(\boldsymbol{x}_k)\right\|. \tag{54}$$

Assumption 2 and compactness of the state space imply that we can bound the gradient of the barrier function by

$$|\nabla_{\boldsymbol{x}}^T\psi(\boldsymbol{x})| \leq C_\psi. \tag{55}$$

By exploiting the Lipschitz continuity of the CBF candidate function $\psi(\cdot)$ and posterior standard deviation $\tilde{\sigma}_g(\cdot)$, we have

$$\begin{aligned}\|\xi_1(\boldsymbol{x}) - \xi_1(\boldsymbol{x_k})\| &\leq \|\boldsymbol{b}\|\sqrt{\beta_g}(C_\psi L_{\sigma_g} + C_{\tilde{\sigma}_g}L_\psi)\|\boldsymbol{x} - \boldsymbol{x}_k\| \\ &= L_{\xi_1}\|\boldsymbol{x} - \boldsymbol{x}_k\|,\end{aligned} \tag{56}$$

where C_{σ_g} denotes upper bound on $\sigma_g(\cdot)$ which is guaranteed to exist since a stationary kernel is assumed to be used in GP regression. Applying the same procedure as for $\xi_1(\cdot)$, we have

$$\begin{aligned}\|\xi_2(\boldsymbol{x}) - \xi_2(\boldsymbol{x_k})\| &\leq \|\boldsymbol{b}\|\,(C_\psi L_{\mu_g} + L_\psi C_{\mu_g})\|\boldsymbol{x} - \boldsymbol{x}_k\| \\ &= L_{\xi_2}\|\boldsymbol{x} - \boldsymbol{x}_k\|.\end{aligned} \tag{57}$$

Analogously, we obtain that

$$\|\xi_3(\boldsymbol{x}) - \xi_3(\boldsymbol{x_k})\| = L_{\xi_3}\|\boldsymbol{x} - \boldsymbol{x}_k\|, \tag{58}$$

where

$$\begin{aligned}L_{\xi_3} &= L_\alpha + C_\psi(\|A\| + \|b\|\,L_{\mu_f} + \|b\|\,\sqrt{\beta_f}L_{\sigma_f}) \\ &\quad + L_\psi(\|A\|\,\bar{\boldsymbol{x}} + \|b\|\,C_{\mu_f} + \|b\|\,\sqrt{\beta_f}C_{\sigma_f}).\end{aligned} \tag{59}$$

Combining the Lipschitz bounds (56), (57), (58), we obtain

$$\begin{aligned}&\xi_1(\boldsymbol{x}(t))|u|\xi_2(\boldsymbol{x}(t))u - \xi_3(\boldsymbol{x}(t)) \leq \\ &\quad \xi_1(\boldsymbol{x}_k)|u| + \xi_2(\boldsymbol{x}_k)u - \xi_3(\boldsymbol{x}_k) \\ &\quad + ((L_{\xi_1}|u| + L_{\xi_2})|u| + L_{\xi_3})\|\boldsymbol{x}_k - \boldsymbol{x}(t)\|.\end{aligned} \tag{60}$$

It remains to bound the state difference $\|\boldsymbol{x}_k - \boldsymbol{x}(t)\|$ within sampling intervals $[t_k, t_k + T)$. For notational simplicity, we denote the bound on the posterior mean function $\mu_f(\cdot)$ by

$$\mu_f(\boldsymbol{x}) \leq \bar{f} + \sqrt{\beta_f}s_f = C_{\mu_f}, \tag{61}$$

where $\bar{f}$ represents the upper bound on the functions $f(\cdot)$ as defined in Remark 2. Then we exploit the boundedness of $f(\cdot)$, $g(\cdot)$ and u, such that

$$\|\boldsymbol{x}_k - \boldsymbol{x}(t)\| \leq (\bar{f} + \bar{g}\bar{u})(t - t_k), \tag{62}$$

which holds due to Jensen's inequality. Therefore, we obtain the inequality

$$\begin{aligned}&\xi_1(\boldsymbol{x}(t))|u| + \xi_2(\boldsymbol{x}(t))u - \xi_3(\boldsymbol{x}(t)) \leq \\ &\quad \xi_1(\boldsymbol{x}_k)|u| + \xi_2(\boldsymbol{x}_k)u - \xi_3(\boldsymbol{x}_k) + \phi T,\end{aligned} \tag{63}$$

for all $t \in [t_k, t_k + T)$. As a result of this reasoning and the implications of the satisfaction of (25) on the CBF condition (5b), safety follows if (49b) and (49c) are jointly feasible. To show this property, we distinguish two cases based on the value of $\tilde{\xi}_3(\boldsymbol{x})$. First, we consider the case that $\tilde{\xi}_3(\boldsymbol{x}) < 0$. Then, the constraint

$$\xi_1(\boldsymbol{x}_k)|u| + \xi_2(\boldsymbol{x}_k)u - \xi_3(\boldsymbol{x}_k) + \phi T \leq 0 \tag{64}$$

leads to the requirement on the input constraint

$$\bar{u} \geq \frac{|\xi_3(\boldsymbol{x}_k)|}{|\xi_2(\boldsymbol{x}_k)| - \xi_1(\boldsymbol{x}_k)} + \frac{\phi T}{|\xi_2(\boldsymbol{x}_k)| - \xi_1(\boldsymbol{x}_k)}, \tag{65}$$

where the first term defines the maximum control input for the continuous-time controller and the second term describes the increase due to the consideration of inter-sampling effects. In order to bound the numerator, we observe that Assumption 7 with $\zeta_2 = \zeta_1(\bar{f} + 2\sqrt{\beta_f}s_f) + \tilde{\phi}$ guarantees $\xi_3(\boldsymbol{x}) \geq \tilde{\phi}$ when $|\nabla_{\boldsymbol{x}}^T\psi(\boldsymbol{x})\boldsymbol{b}| \leq \zeta_1$. Thus, $\tilde{\xi}_3(\boldsymbol{x}) < 0$ and $T \leq \tilde{\phi}/\phi$ imply $|\nabla_{\boldsymbol{x}}^T\psi(\boldsymbol{x})\boldsymbol{b}| > \zeta_1$, such that we obtain

$$\begin{aligned}|\xi_2(\boldsymbol{x})| - \xi_1(\boldsymbol{x}) &= |\nabla_{\boldsymbol{x}}^T\psi(\boldsymbol{x})\boldsymbol{b}|\left(|\mu_g(\boldsymbol{x})| - \sqrt{\beta_g}\tilde{\sigma}_g(\boldsymbol{x})\right)\\ &\geq \zeta_1\epsilon\sqrt{\beta_g}\tilde{\sigma}_g(\boldsymbol{x})\end{aligned}$$

where the second line follows from (50) and the lower bound $\mu_g(\boldsymbol{x}) \geq \underline{g} - \sqrt{\beta_g}\sigma_g(\boldsymbol{x})$. This inequality directly leads to the input bound restriction

$$\bar{u} \geq \frac{\max_{\boldsymbol{x}\in\mathcal{C}} \xi_3(\boldsymbol{x})}{\zeta_1\epsilon\sqrt{\beta_g}\underline{\sigma}_g} + \frac{\phi T}{\zeta\epsilon\sqrt{\beta_g}\underline{\sigma}_g}. \tag{66}$$

As the second summand is linear in T, the feasibility is ensured by (52) and a sufficiently small sampling time T. In order to obtain the upper bound for these sufficiently small sampling times T, we solve (66) for T, which yields (51) and concludes the first case. In the second case, we consider $\tilde{\xi}_3(\boldsymbol{x}) \geq 0$, such that the constraint (64) leads to a requirement on the input constraint of the form

$$|u| \leq \frac{|\xi_3(\boldsymbol{x}_k)|}{|\xi_2(\boldsymbol{x}_k)| - \xi_1(\boldsymbol{x}_k)} + \frac{\phi T}{|\xi_2(\boldsymbol{x}_k)| - \xi_1(\boldsymbol{x}_k)}, \tag{67}$$

where the absolute value on $|u|$ is resolved depending on the sign of $\xi_1(\boldsymbol{x})$. Since constraints of this form always include the trivial solution $u = 0$, feasibility is always guaranteed. Therefore, feasibility is ensured if the conditions (52) and (51) based on the first case are satisfied. ■

In comparison to the continuous-time result in Proposition 1, the tightened condition (50) for the posterior GP is required. This necessity arises due to the additional requirement for compliance with the input constraint (49c), since it can be straightforwardly seen that for $\epsilon \to 0$, the right-hand side of (52) diverges to ∞. Thus, Proposition 4 has the intuitive interpretation that a more accurate GP model generally admits smaller control input bounds $\bar{u}$. For the sampling time constraint (51), the interpretation is also straightforward. On the one hand, smaller Lipschitz constants L_{ξ_i} imply slower varying safety conditions and thus, generally admit larger sampling times T. Larger margins $\tilde{\phi}$ have a similar effect. An increase of the input bound $\bar{u}$ allows larger sampling times T when it is close to the admissible minimum value $\max_{\boldsymbol{x}\in\mathcal{C}} \xi_3(\boldsymbol{x})/\zeta_1\epsilon\sqrt{\beta_g}\underline{\sigma}_g$, but causes a reduction when $\bar{u}$ is significantly larger than this value. This effect is caused by the quadratic dependency of ϕ on $\bar{u}$, which overcomes the linear growth in (51). Thereby, this behavior intuitively captures the effect that excessive control

Algorithm 2 Safe Online Learning for Sampled-Data Systems

$N \leftarrow 0$, $k \leftarrow 0$, $t \leftarrow 0$
compute β_f using (12a)
determine β_g, $\underline{\sigma}_g$ by solving (31) and $\underline{u}_{\mathrm{GP}}$ based on (33)
while true do
  if $t < kT$ **then**
    apply u
  else
    compute safety-filtered control u_k using (49)
    $k \leftarrow k + 1$
    if $\frac{\sqrt{\beta}\sigma_g(\boldsymbol{x}_k)}{\mu_g(\boldsymbol{x}_k)} \leq 1 + \epsilon + \gamma$ **then**
      $N \leftarrow N + 1$
      compute excitation control $\bar{u}_k$ using (68)
      set $u = \bar{u}_k$ and apply u
      measure $y = f(\boldsymbol{x}_k) + g(\boldsymbol{x}_k)u + \omega$
      $\mathbb{D} \leftarrow \mathbb{D} \cup \{([\boldsymbol{x}_k^T, u]^T, y\}$
      update $\mu_f(\cdot)$, $\mu_g(\cdot)$, $\sigma_f(\cdot)$, $\sigma_g(\cdot)$
    else
      set $u = u_k$ and apply u
    end if
  end if
end while

inputs can cause a significant change in the system state within a very short amount of time, but a sufficiently large control input is necessary to account for the negative effects of sampled-data control.

Remark 6: Control input constraints (49c) are *necessary* in contrast to the continuous-time analysis in Section III to bound the effect of control on the system over a finite interval of time. Since these constraints can potentially cause feasibility issues, the bound $\bar{u}$ needs to be selected sufficiently large to admit the control inputs required for ensuring safety, which is ensured via (52). Note that it is straightforward to also consider input bounds satisfying (52) for the results in Section III.

B. Event-Triggered Learning in Sampled-Data Systems

Similarly to Section III-D, we augment the GP-based safe control law (49) using an event-triggered learning to avoid the requirement of a priori satisfaction of (50). Since the guarantees of Proposition 2 transfer to the sampled-data control scenario, we can use it as excitation filter. Using the sampled-data control law (49), the resulting control law reads as

$$\bar{u}_k = \begin{cases} u_k & \text{if } |u_k| \geq \underline{u}_{\mathrm{GP}} \\ -\mathrm{sgn}(\tilde{\xi}_s(\boldsymbol{x}_k))\underline{u}_{\mathrm{GP}} & \text{else.} \end{cases} \tag{68}$$

Based on this definition, we can distinguish again between the learning and control focused phases of the overall control law:

- The excitation filter should be applied only when accuracy of $\mu_g(\cdot)$ is necessary. Therefore, we activate the excitation filter (68) by a sampled-data event trigger

$$t_{N+1} = \inf_{kT > t_N} kT \tag{69a}$$

$$\text{such that } \frac{\mu_g(\boldsymbol{x}(kT))}{\sqrt{\beta_g}\sigma_g(\boldsymbol{x}(kT))} \leq 1 + \epsilon + \gamma, \tag{69b}$$

such that we employ the control signal

$$u(t) = \bar{u}_k, \quad \forall t \in [t_{N+1}, t_{N+1} + T), N \in \mathbb{N}, \tag{70}$$

to obtain a new training data sample $([\boldsymbol{x}^T(t_{N+1}), \bar{u}_k]^T, y)$ with $k = \frac{t_{N+1}}{T}$.

- When the model accuracy is sufficient, we employ the safe control law (49), resulting in

$$u(t) = u_k, \quad \forall t \in [t_k, t_{k+1}), k \in \mathbb{N}, k \neq \frac{t_N}{T}, N \in \mathbb{N}. \tag{71}$$

Note that the event trigger (69) is restricted to sampling times kT, $k \in \mathbb{N}$, since the sampled-data realization of the control law prevents us from taking measurements at arbitrary times. To account for this restriction, the sampling occurs preemptively using the tightened threshold $1+\epsilon+\gamma$ compared to (40). The resulting procedure is summarized in Algorithm 2, for which the safety guarantees from the continuous-time scenario can be maintained as shown in the following result.

Theorem 2: Consider a system (1) with sampled-data control constraint (6), GP priors (8a), (8b), and a control barrier function $\psi(\cdot)$ inducing a bounded safe set $\mathcal{C}$ such that Assumptions 1 - 7 are satisfied with $\zeta_2 = \zeta_1(\bar{f} + 2\sqrt{\beta_f} s_f) + \tilde{\phi}$, $\tilde{\phi} \in \mathbb{R}_{>0}$, in (17). Moreover, assume that $s_g > \underline{\sigma}_g$. Then, for all $N \in \mathbb{N}$, Algorithm 2 with design parameters $\epsilon, \gamma \in \mathbb{R}_{>0}$ and ϕ defined in (53) yields a well-defined control law and guarantees safety during the time interval $[t_N, t_{N+1})$ with probability of at least $1 - \delta$ if

$$\bar{u} > \max\left\{ \underline{u}_{\mathrm{GP}}, \frac{\max_{\boldsymbol{x} \in \mathcal{C}} \xi_3(\boldsymbol{x})}{\zeta_1 \epsilon \sqrt{\beta_g} \underline{\sigma}_g} \right\} \tag{72}$$

$$\gamma \geq L_\Gamma T, \tag{73}$$

and (51) hold, and (19) and $x(t) \in \mathcal{C}$ are satisfied at $t = t_N$.

Proof: Whenever $\mu(\boldsymbol{x}_k)/\sqrt{\beta_g}\tilde{\sigma}_g(\boldsymbol{x}_k) \geq 1 + \epsilon + \gamma$, (73) and Proposition 3 guarantee that (50) holds until the next time step $k + 1$. If this condition is not satisfied, the exciting control input is applied and a new data point is generated, such that Proposition 2 guarantees $\mu(\boldsymbol{x}_k)/\sqrt{\beta_g}\tilde{\sigma}_g(\boldsymbol{x}_k) \geq 1 + \epsilon + \gamma$ for the updated GP model. Hence, (50) is also satisfied until the next time step $k + 1$. Therefore, it follows from (51), (72), Proposition 4 and the straightforward adaptation of Proposition 2 to the sampled-data control setting that the control law is well-defined and guarantees safety during the time interval $[t_N, t_N + 1)$, for $N \in \mathbb{N}$. ■

This result transfers the guarantees from the continuous-time controller outlined in Algorithm 1 to the sampled-data case. Due to the necessity of input constraints, this transfer can only be achieved under additional restrictions. Similarly to Proposition 4, the control input bound must be sufficiently large as defined in (72), which in the event-triggered learning scheme also requires the admissibility of the control input $\underline{u}_{\mathrm{GP}}$ necessary for sufficiently exciting the system. Moreover, the upper bound (51) from Proposition 4 is inherited. Finally, the inter-event time must admit the realizability of the GP updates under the sampled-data paradigm, i.e., the inter-event times Δ_i must be larger than the sampling time T, which induces (73). Therefore, the additional conditions of Theorem 2 compared to Theorem 1 intuitively follow from the sampled-data realization and can generally be satisfied straightforwardly by choosing a sufficiently large value $\bar{u}$ and a sufficiently small sampling time T.

V. Numerical Evaluation in Adaptive Cruise Control

In order to demonstrate the effectiveness of the derived theory, we consider its application in the example of an adaptive cruise control. In Section V-A, we evaluate our proposed framework on continuous-time controllers. The extenstion to sampled-data systems is discussed in Section V-B.

A. Safe Control in Continuous Time

We demonstrate the effectiveness of our framework by considering the example of adaptive cruise control as presented, e.g., in [17]. To enable the straightforward applicability of the proposed theory, we represent the dynamics as

$$\underbrace{\begin{bmatrix}\dot{\tilde{v}} \\ \dot{z}\end{bmatrix}}_{\dot{\boldsymbol{x}}} = \underbrace{\begin{bmatrix}0 & 0 \\ -1 & 0\end{bmatrix}}_{\boldsymbol{A}} \boldsymbol{x} + \underbrace{\begin{bmatrix}1 \\ 0\end{bmatrix}}_{\boldsymbol{b}} \Bigg(\underbrace{-\frac{F_r(\tilde{v})}{m}}_{f(\boldsymbol{x})} + \underbrace{\frac{2(1+\frac{1}{2}sin(\frac{v}{2}))}{m}}_{g(\boldsymbol{x})} u \Bigg), \tag{74}$$

where the state $\boldsymbol{x} = \begin{bmatrix}\tilde{v} & z\end{bmatrix}^T \in \mathbb{R}^2$ is composed of the distance to the front vehicle z and the difference $\tilde{v} = v - v_0$ between the ego vehicle velocity v and a front vehicle's velocity v_0, which we assume to be constant and known. The parameter $m = 1650$ corresponds to the ego vehicle's mass and $F_r(\tilde{v}) = f_0 + f_1(\tilde{v} + v_0) + f_2(\tilde{v} + v_0)^2$ is the rolling resistance force on the ego vehicle with parameters $f_0 = 0.2$, $f_1 = 10$ and $f_2 = 0.5$. Note that we employ a modification of the original dynamics considered in [17] by defining a state-dependent function $g(\cdot)$ instead of a constant in order to render the problem slightly more challenging. This change does not have an impact on the structure of the problem, such that it exhibits the form (1) regardless of the choice of positive definite functions $g(\cdot)$. The objective is to reach the desired velocity v_d, for which we design a nominal velocity controller $\pi_{\mathrm{nom}}(\boldsymbol{x}) = -2000(v - v_d)$. Since it is crucial that no collision with the front vehicle occurs, we define a CBF

$$\psi(\boldsymbol{x}) = z - T_h(\tilde{v} + v_0), \tag{75}$$

where $T_h = 1.8$ is the lookahead time. Moreover, we use $\alpha(\psi) = 65\psi$. As we assume that the functions $f(\cdot)$ and $g(\cdot)$ are unknown, we model their behavior by putting a prior GP distribution $\mathcal{GP}(0, k_f(\cdot,\cdot))$ and $\mathcal{GP}(0, k_g(\cdot,\cdot))$ on them. For $k_f(\cdot,\cdot)$ and $k_g(\cdot,\cdot)$, we employ the squared exponential kernel, whose hyperparameters are set to $l_f = 1$, $l_g = 2$, $s_f = 0.1$, $s_g = 4 \cdot 10^{-4}$. In order to comply with the required feasibility of the CBF condition at $t = 0$ in Theorem 1, we initialize the composite GP model (10a) - (10d) with one training point before starting Algorithm 1. All training samples that we obtain through our proposed framework are perturbed by Gaussian noise with standard deviation $\sigma_{\mathrm{on}} = 0.01$. Furthermore, we choose sufficiently small values $\tau_f = 10^{-6}$ and $\tau_g = 10^{-6}$ for computing (12a) and (12b), such that (31) with $\delta = 0.01$ can be satisfied by solving for $\underline{\sigma}_g$. When executing Algorithm 1, we employ the conservative prior bounds $\underline{g} = \frac{1}{2000}$ and $\overline{g} = \frac{3}{1000}$ and choose $\epsilon = 0.2$ and $\gamma = 0.5$ for the design parameters. To demonstrate the effectiveness of the proposed safe control approach through event-triggered learning, we apply Algorithm 1 in a setting with conflicting goals of the nominal controller $\pi_{\mathrm{nom}}(\cdot)$ and the safety conditions by setting $v_0 = 14$ and $v_d = 24$, i.e., the desired velocity v_d is higher than the front vehicle's velocity v_0. The resulting state trajectories are depicted in Fig. 2. In the top plot, we observe that the velocity of the vehicle steadily approaches v_d until there is a noticeable reduction in distance, as shown in the bottom plot. Due to the CBF, the speed of the vehicle converges to the speed of the ego vehicle v_0, while ensuring a safe distance. This distance can be directly quantified using the definition of the CBF in (75), which yields $T_h v_0 = 25.2$. This behavior can be observed independently of the prior availability of exact model knowledge, which is due to our proposed strategy for event-triggered learning strategy. As depicted at the top of Fig. 3, the triggering condition (40) generates data at an almost constant rate at the beginning in order to achieve the necessary model accuracy. For ensuring a sufficient information gain with each of these samples, the magnitude of the control input resulting from the CBF-QP (20) is adapted in the safe direction after it drops below the excitation threshold $\bar{u}_{\mathrm{GP}}$. Note that Algorithm 1 not only triggers update events when close to the constraint boundary as maintaining the feasibility of the CBF-QP (20) is crucial regardless of our distance from the boundary. When the dynamical system has almost reached a stationary point after $t = 13$, the triggering stops. Thereby, merely 116 data points are necessary to ensure safety using our event-triggered learning approach. This is in strong contrast to a time-triggered online version without excitation filter. It can be clearly seen at the top of Fig. 3 that periodically updating the GP model cannot ensure feasibility of the CBF-SOCP, which causes a diverging trajectory and constraint violations after $\approx 6s$. As illustrated at the bottom of Fig. 3, Algorithm 1 achieves these safety guarantees without excessive cautiousness: The CBF converges to a value very close to the safety threshold $\psi(\boldsymbol{x}) = 0$, but continuously stays above it. Therefore, this example clearly illustrates the effectiveness and data-efficiency of ensuring safety using Algorithm 1.

Additionally, we analyze the influence of parameters on the number of triggering events during the first 8s of the simulation, where our focus is primarily on learning and triggers occur more frequently. We first investigate how the trade-off between control effort and number of trigger events depends on the design parameter γ by running 100 simulations per choice of γ with the nominal parameters values for v_0, $\boldsymbol{x}_0$ and v_d perturbed by value randomly sampled from a uniform distribution over $[-2, 2]$. As shown in Fig. 4, increasing γ causes growing control inputs $\underline{u}_{\mathrm{GP}}$, while simultaneously reducing the number of sampled data points. This behavior arises because higher control inputs provide more information about $g(\cdot)$, thus requiring fewer data points to sufficiently reduce the uncertainty for guaranteeing (19). Furthermore, the increase in the value of the signal variance s_g^2 of the kernel function of the GP leads to a decrease in triggering events, as depicted in the Figure 5. Using larger values of s_g^2 requires higher control inputs $\underline{u}_{\mathrm{GP}}$ due to (33), such that more information can be gathered from a single data point and fewer training samples is sufficient. Lastly, the effect of the length scale on the number of triggering events is shown in Figure 6. As observed, increasing the lengthscale of the GP process will lead to a decrease in the number of triggering events since the uncertainty grows slower with the distance to the closest training data point. Note that an increase in the noise variance σ_{on}^2 does not change the qualitative behaviors, but mainly causes an increase in the necessary control inputs $\underline{u}_{\mathrm{GP}}$, which simultaneously reduces the number of trigger events N_{tr}.

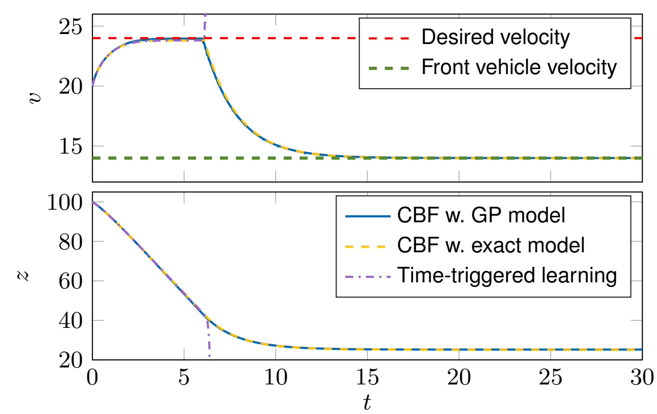

Fig. 2. The continuous-time control approach in Algorithm 1 with event-triggered online learning results in almost identical state trajectories as a CBF-based controller with exact model knowledge in contrast to an analogous approach with periodically updated GP model, which becomes infeasible after $\approx 6s$. Top: The velocity of the ego vehicle approaches its desired value v_d at the beginning, but eventually converges toward the front car's velocity v_0 to preserve a safe distance. Bottom: The distance to the front vehicle decays continuously until a safety distance of approximately $T_h v_0 = 25.2$ is maintained.

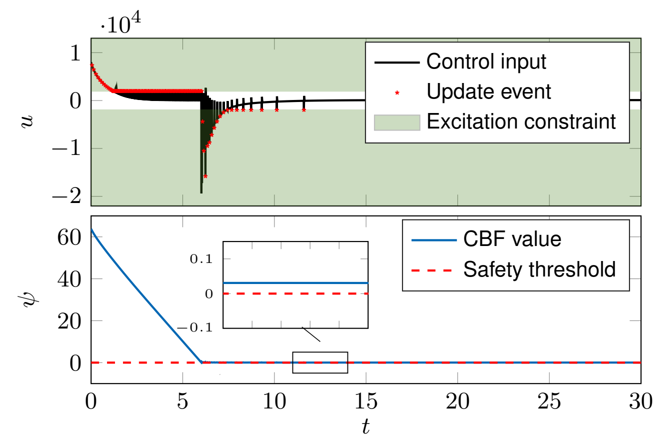

Fig. 3. The event-triggered update scheme in Algorithm 1 ensures the necessary model accuracy for guaranteeing safety by sampling data until the system state has converged and the model can be kept unchanged. Top: When the control input resulting from the CBF-QP (20) is not large enough to provide sufficient information for the GP update, the excitation filter (32) magnifies it in a safe direction such that the excitation threshold $\underline{u}_{\mathrm{GP}}$ is exceeded. Bottom: The value of the control barrier function approaches its safety threshold $\psi(\boldsymbol{x}) = 0$ but never falls below it, which illustrates the safety guarantees of Algorithm 1.

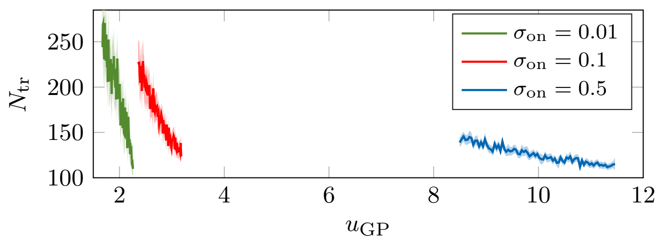

Fig. 4. The average number of triggering events N_{tr} based on the different values of the excitation filter $\underline{u}_{GP}$ evaluated on 100 trajectories with randomized simulation setting.

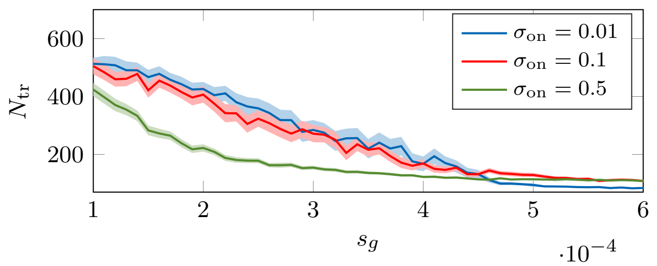

Fig. 5. The average number of triggering events N_{tr} based on the different values of the signal variance s_g of a GP model evaluated on 100 trajectories with randomized simulation setting.

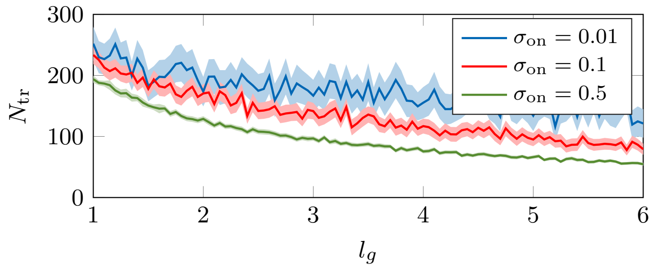

Fig. 6. The average number of triggering events N_{tr} based on the different values of the lengthscale l_g of a GP model evaluated on 100 trajectories with randomized simulation setting.

B. Safe Sampled-Data Control

In order to investigate the behavior of the presented approach for safe event-triggered learning in sampled-data systems, we adopt the setting from Section V-A, introducing additional necessary parameters for our proposed theory. From Assumption 1, the function $f(\cdot)$ is bounded, and we set the upper bound to $\bar{f} = 49000$. In order to ensure feasibility, we introduce input constraints and set $\bar{u} = 20000$.

Based on these parameters, we run Algorithm 2 with sampling time $T = 0.01$, which leads to the results depicted in Fig. 7. While the general behavior of the state trajectories look similar to the continuous-time scenario illustrated in Fig. 2, minor differences can be observed. Due to the tightened safety conditions in the sampled-data scenario, the ego vehicle keeps a slightly larger distance to the vehicle in front of it. This is an intuitive effect since it effectively gives the controller extra time to react since control updates are only possible at sampling times. Moreover, it is clearly visible that the ego vehicle does not reach the desired vehicle, even

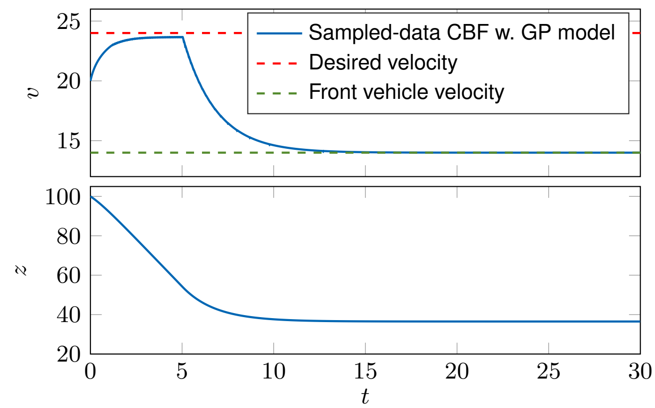

Fig. 7. The sampled-data control approach Algorithm 2 with sampling time $T = 0.01$ ensures safety in a practically realizable setting with a similar performance as the continuous time approach. Top: Due to the tightened safety conditions in the sampled-data case, the ego vehicle does not reach the desired velocity even when far away from the front vehicle. Bottom: The increased conservatism is also visible in the asymptotic distance to the target vehicle, which remains considerably larger than in the continuous-time control approach.

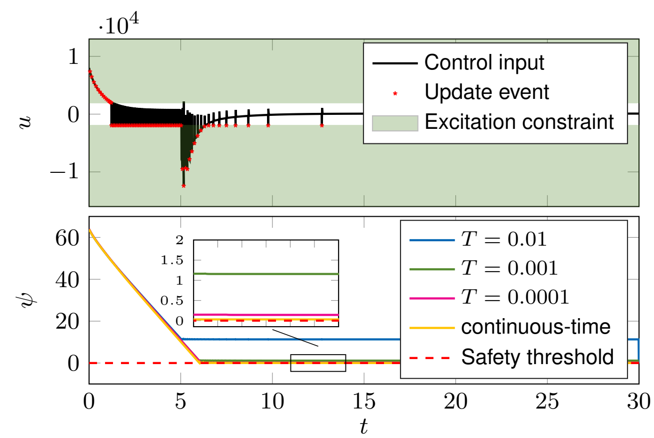

Fig. 8. By increasing the robustness of the CBF conditions depending on the sampling time T, Algorithm 2 provides an adaptive conservatism converging to the continuous-time behavior for $T \to 0$. Top: For a comparatively large sampling time $T = 0.01$, the constraint tightening necessary to account for inter-sampling effects can cause the excitation filter to change the sign of control inputs compared to the continuous-time scenario. Bottom: Larger sampling times T require a higher cautiousness, such that the achievable proximity to the safety threshold $\psi(\boldsymbol{x}) = 0$ increases with T.

when the distance to the front vehicle is large. While this effect is not so intuitive, it can be easily explained when looking at the applied control inputs depicted at the top of Fig. 8. Due to the tightened CBF constraints to account for inter-sampling effects, the excitation filter yields negative control inputs, which causes the visible reduction in velocity compared to the continuous-time controller. These negative effects of the sampled-data implementation can be reduced by decreasing the sampling time T as illustrated at the bottom of Fig. 8. While a significant distance to the safety threshold $\psi(\boldsymbol{x}) = 0$ is visible for $T = 0.01$, it continuously reduces such that barely any difference exists between the continuous-time realization and the sampled-data implementation with

$T = 0.0001$. Since the number of triggered update events remains almost unaffected with a total of 77 triggers in this setting, the sampled-data approach in Algorithm 2 provides us with a straightforward and practically implementable way to ensure safety using data-efficient online learning.

VI. Conclusions

We have presented a novel approach for safe control through GP-based event-triggered learning in a partially unknown environments. For achieving this, we first introduce robust CBF conditions for ensuring the safety of unknown dynamical systems evolving continuously in time when only a GP model is available. Based on these conditions, we design strategic triggers, which update the model using data generated online, such that they provide a sufficient excitation to efficiently reduce uncertainty. Since controllers typically need to be implemented in a sampled-data fashion, we extend the method to account for inter-sampling effect. Safety guarantees for the resulting online learning control approach and the absence of Zeno behavior with the proposed triggering scheme are formally shown. The effectiveness of our theoretical results is demonstrated in numerical simulations of an adaptive cruise control system. Future work will focus on extending the proposed framework to more general classes of system dynamics and validating our results in hardware experiments.

Appendix

Lemma 3: Consider a control input $u \in \mathbb{R}$ and constants $c_1 \in \mathbb{R}_{>0}$, and $c_2, c_3 \in \mathbb{R}$, such that $c_1 < |c_2|$. Then,

$$c_1|u| + c_2 u \leq c_3 \tag{76}$$

is equivalent to the condition

$$(\mathrm{sgn}\,(c_2 c_3)\, c_1 + c_2)\, u \leq c_3. \tag{77}$$

Proof: We can resolve the absolute value in (76) by considering two cases based on the sign of the control input:

$$1)\ u \geq 0: \quad c_1|u| + c_2 u \leq c_3 \Leftrightarrow (c_1 + c_2)u \leq c_3 \tag{78}$$

$$2)\ u < 0: \quad c_1|u| + c_2 u \leq c_3 \Leftrightarrow (-c_1 + c_2)u \leq c_3 \tag{79}$$

It remains to unify these two cases into a single equation again. For this purpose, we consider four different cases based on the signs of the constants c_2 and c_3:

1) $c_2 \geq 0$ and $c_3 \geq 0$: Given the conditions $c_2 \geq 0$ and $c_1 < |c_2|$, it follows that $(-c_1+c_2) > 0$. Therefore, (76) is satisfied for all $u < 0$ as $c_3 \geq 0$. This implies that the constraint (79) is redundant in this case. It can directly be seen that (78) is not redundant in this case since for u sufficiently large, it is not satisfied anymore. Finally, $(c_1 + c_2) > 0$, such that (78) is also redundant for $u < 0$. Therefore, (76) is equivalent to (78) for all $u \in \mathbb{R}$ in this case.

2) $c_2 \leq 0$ and $c_3 \leq 0$: Given the conditions $c_2 < 0$ and $c_1 < |c_2|$, it follows that $(c_1 + c_2) < 0$. As $c_3 \leq 0$, (79) cannot be satisfied by any control input $u < 0$. Similarly, we have $(-c_1+c_2) < 0$ such that (78) cannot be satisfied for any control input $u < 0$. Thus, both constraints are equivalent for $u < 0$. For $u > 0$, only (78) needs to be satisfied, which can easily be checked to be a non-trivial constraint. Hence, we can equivalently express (76) as (78) for all $u \in \mathbb{R}$ in this case.

3) $c_2 \geq 0$ and $c_3 \leq 0$: Analogous to case 1, we have $(c_1 + c_2) > 0$. Given that $c_3 \leq 0$, it can be straightforwardly seen that no control input $u > 0$ can satisfy (78). Moreover, we also have $(-c_1+c_2) > 0$, such that also no control input $u > 0$ can satisfy (79). In other words, both constraints are equivalent for $u > 0$. However, for $u < 0$, only (79) needs to be satisfied and can easily be shown to be non-trivial. Therefore, (76) is equivalent to (79) for all $u \in \mathbb{R}$ in this case.

4) $c_2 \leq 0$ and $c_3 \geq 0$: In the final case, we have, analogously to case 2, $(c_1 + c_2) < 0$. Given that $c_3 \geq 0$, any control input $u > 0$ automatically satisfies (78), rendering it redundant. As $(-c_1 + c_2) < 0$, (79) is also redundant for $u < 0$. However, it can easily be checked that for $u < 0$ it is non-trivial, such that we can equivalently express (76) as (79) for all $u \in \mathbb{R}$.

Combining all these cases, we obtain

$$c_1\|u\| + c_2 u \leq c_3 \Leftrightarrow \begin{cases} c_2 \geq 0 \text{ and } c_3 \geq 0, & (c_1+c_2)u \leq c_3 \\ c_2 \leq 0 \text{ and } c_3 \leq 0, & (c_1+c_2)u \leq c_3 \\ c_2 \geq 0 \text{ and } c_3 \leq 0, & (-c_1+c_2)u \leq c_3 \\ c_2 \leq 0 \text{ and } c_3 \geq 0, & (-c_1+c_2)u \leq c_3. \end{cases}$$

Since the case distinction depends only on c_2 and c_3, we can equivalently formulate it in a compact form through (77). ■

References

[1] C. E. Rasmussen and C. K. I. Williams, *Gaussian Processes for Machine Learning*. Cambridge: The MIT Press, 2006.

[2] A. Lederer, J. Umlauft, and S. Hirche, "Uniform error bounds for Gaussian process regression with application to safe control," in *Advances in Neural Information Processing Systems*, pp. 659–669, 2019.

[3] N. Srinivas, A. Krause, S. M. Kakade, and M. W. Seeger, "Information-Theoretic Regret Bounds for Gaussian Process Optimization in the Bandit Setting," *IEEE Transactions on Information Theory*, vol. 58, no. 5, pp. 3250–3265, 2012.

[4] P. Jagtap, G. J. Pappas, and M. Zamani, "Control barrier functions for unknown nonlinear systems using Gaussian processes," in *Proceedings of the IEEE Conference on Decision and Control*, pp. 3699–3704, 2020.

[5] K. Long, V. Dhiman, M. Leok, J. Cortés, and N. A. Atanasov, "Safe control synthesis with uncertain dynamics and constraints," *IEEE Robotics and Automation Letters*, vol. 7, pp. 7295–7302, 2022.

[6] A. Lederer, A. Begzadić, N. Das, and S. Hirche, "Safe learning-based control of elastic joint robots via control barrier functions," *IFAC-PapersOnLine*, vol. 56, no. 2, pp. 2250–2256, 2023. 22nd IFAC World Congress.

[7] P. Mestres and J. Cortés, "Feasibility and regularity analysis of safe stabilizing controllers under uncertainty," *Automatica*, vol. 167, p. 111800, 2024.

[8] F. Castañeda, J. J. Choi, B. Zhang, C. J. Tomlin, and K. Sreenath, "Pointwise feasibility of Gaussian process-based safety-critical control under model uncertainty," in *Proceedings of the IEEE Conference on Decision and Control*, pp. 6762–6769, 2021.

[9] R. Goebel, R. G. Sanfelice, and A. R. Teel, *Hybrid Dynamical Systems: Modeling, Stability, and Robustness*. Princeton: Princeton University Press, 2012.

[10] Y. Fan, L. Liu, G. Feng, and Y. Wang, "Self-triggered consensus for multi-agent systems with zeno-free triggers," *IEEE Transactions on Automatic Control*, vol. 60, pp. 2779–2784, 2015.

[11] W. Shaw Cortez, D. Oetomo, C. Manzie, and P. Choong, "Control Barrier Functions for Mechanical Systems: Theory and Application to Robotic Grasping," *IEEE Transactions on Control Systems Technology*, vol. 29, no. 2, pp. 530–545, 2021.

[12] J. L. Breeden, K. Garg, and D. Panagou, "Control barrier functions in sampled-data systems," *IEEE Control Systems Letters*, vol. 6, pp. 367–372, 2021.

[13] V. Dhiman, M. J. Khojasteh, M. Franceschetti, and N. Atanasov, "Control Barriers in Bayesian Learning of System Dynamics," *IEEE Transactions on Automatic Control*, vol. 68, no. 1, pp. 214–229, 2023.

[14] F. Solowjow, D. Baumann, J. Garcke, and S. Trimpe, "Event-triggered learning for resource-efficient networked control," in *Proceedings of the American Control Conference*, pp. 6506–6512, 2018.

[15] J. Umlauft and S. Hirche, "Feedback linearization based on Gaussian processes with event-triggered online learning," *IEEE Transactions on Automatic Control*, vol. 65, pp. 4154–4169, 2019.

[16] J. Jiao, A. Capone, and S. Hirche, "Backstepping tracking control using Gaussian processes with event-triggered online learning," *IEEE Control Systems Letters*, vol. 6, pp. 3176–3181, 2022.

[17] A. D. Ames, X. Xu, J. W. Grizzle, and P. Tabuada, "Control Barrier Function Based Quadratic Programs for Safety Critical Systems," *IEEE Transactions on Automatic Control*, vol. 62, no. 8, pp. 3861–3876, 2017.

[18] F. Castañeda, J. J. Choi, W. Jung, B. Zhang, C. J. Tomlin, and K. Sreenath, "Recursively feasible probabilistic safe online learning with control barrier functions," *arXiv preprint arXiv:2208.10733*, 2023.

[19] J. J. Choi, F. Castañeda, W. Jung, B. Zhang, C. J. Tomlin, and K. Sreenath, "Constraint-guided online data selection for scalable data-driven safety filters in uncertain robotic systems," *arXiv preprint arXiv:2311.13824*, 2023.

[20] A. Capone, R. K. Cosner, A. Ames, and S. Hirche, "Safe online dynamics learning with initially unknown models and infeasible safety certificates," *arXiv preprint arXiv:2311.02133*, 2023.

[21] H. K. Khalil, *Nonlinear systems; 3rd ed.* Upper Saddle River, NJ: Prentice-Hall, 2002.

[22] Q. Nguyen and K. Sreenath, "Exponential control barrier functions for enforcing high relative-degree safety-critical constraints," in *Proceedings of the American Control Conference*, pp. 322–328, 2016.

[23] W. Xiao and C. Belta, "Control barrier functions for systems with high relative degree," *Proceedings of the IEEE Conference on Decision and Control*, pp. 474–479, 2019.

[24] M. Greeff, A. W. Hall, and A. P. Schoellig, "Learning a Stability Filter for Uncertain Differentially Flat Systems using Gaussian Processes," in *Proceedings of the IEEE Conference on Decision and Control*, pp. 789–794, 2021.

[25] T. Beckers, D. Kulić, and S. Hirche, "Stable Gaussian Process based Tracking Control of Euler-Lagrange Systems," *Automatica*, vol. 103, no. 23, pp. 390–397, 2019.

[26] M. Greeff and A. P. Schoellig, "Exploiting differential flatness for robust learning-based tracking control using Gaussian processes," *IEEE Control Systems Letters*, vol. 5, no. 4, pp. 1121–1126, 2021.

[27] A. Lederer, *Gaussian Processes in Control: Performance Guarantees through Efficient Learning*. PhD thesis, Technische Universität München, 2023.

[28] C. A. Micchelli, Y. Xu, and H. Zhang, "Universal kernels," *Journal of Machine Learning Research*, vol. 7, pp. 2651–2667, 2006.

[29] A. Lederer, A. Capone, J. Umlauft, and S. Hirche, "How training data impacts performance in learning-based control," *IEEE Control Systems Letters*, vol. 5, pp. 905–910, 2021.

[30] D. K. Duvenaud, *Automatic Model Construction with Gaussian Processes*. PhD thesis, University of Cambridge, 2014.

[31] A. Lederer, A. Ordonez Conejo, K. Maier, W. Xiao, J. Umlauft, and S. Hirche, "Gaussian Process-Based Real-Time Learning for Safety Critical Applications," in *Proceedings of the International Conference on Machine Learning*, pp. 6055–6064, 2021.

[32] F. Blanchini and S. Miani, *Set-Theoretic Methods in Control*. Boston, MA: Birkhäuser Boston, 2008.

[33] E. A. Coddington and N. Levinson, *Theory of Ordinary Differential Equations*. McGraw-Hill, 1955.

Armin Lederer (S'20, M23) received the B.Sc. and M.Sc. degree in electrical engineering and information technology from the Technical University of Munich, Munich, Germany, in 2015 and 2018, respectively. From 2018 until 2023, he has been a PhD student at the Chair of Information-oriented Control, Department of Electrical and Computer Engineering at the Technical University of Munich, Germany. Since 2023 he is a postdoctoral researcher in the Learning & Adaptive Systems Group at ETH Zurich, Switzerland. His current research interests include the stability of data-driven control systems and machine learning in closed-loop systems.

Azra Begzadić (S'23) received her B.Sc. degree from Vienna University of Technology, Austria, and her M.Sc. degree in electrical engineering and information technology from the Technical University of Munich, Germany, in 2020 and 2023, respectively. She is currently pursuing her Ph.D. degree in Mechanical and Aerospace Engineering at the University of California, San Diego. Her research interests lie in safety-critical learning-based control.

Sandra Hirche (M'03, SM'11, F'20) received the Dipl.-Ing degree in aeronautical engineering from the Technical University of Berlin, Berlin, Germany, in 2002, and the Dr. Ing. degree in electrical engineering from the Technical University of Munich, Munich, Germany, in 2005. From 2005 to 2007, she was awarded a Postdoctoral scholarship from the Japanese Society for the Promotion of Science at the Fujita Laboratory, Tokyo Institute of Technology, Tokyo, Japan. From 2008 to 2012, she was an Associate Professor with the Technical University of Munich. Since 2013, she has served as Technical University of Munich Liesel Beckmann Distinguished Professor and has been with the Chair of Information-Oriented Control, Department of Electrical and Computer Engineering, Technical University of Munich. She has authored or coauthored more than 150 papers in international journals, books, and refereed conferences. Her main research interests include cooperative, distributed, and networked control with applications in human–machine interaction, multirobot systems, and general robotics. Dr. Hirche has served on the editorial boards of the IEEE Transactions on Control of Network Systems, the IEEE Transactions on Control Systems Technology, and the IEEE Transactions on Haptics. She has received multiple awards such as the Rohde & Schwarz Award for her Ph.D. thesis, the IFAC World Congress Best Poster Award in 2005, and – together with students – the 2018 Outstanding Student Paper Award of the IEEE Conference on Decision and Control.

Jorge Cortés (M'02, SM'06, F'14) received the Licenciatura degree in mathematics from Universidad de Zaragoza, Zaragoza, Spain, in 1997, and the Ph.D. degree in engineering mathematics from Universidad Carlos III de Madrid, Madrid, Spain, in 2001. He held postdoctoral positions with the University of Twente, Twente, The Netherlands, and the University of Illinois at Urbana-Champaign,Urbana, IL, USA. He was an Assistant Professor with the Department of Applied Mathematics and Statistics, University of California, Santa Cruz, CA, USA, from 2004 to 2007. He is a Professor and Cymer Corporation Endowed Chair in High Performance Dynamic Systems Modeling and Control at the Department of Mechanical and Aerospace Engineering, University of California, San Diego, CA, USA. He is a Fellow of IEEE, SIAM, and IFAC. His research interests include distributed control and optimization, network science, nonsmooth analysis, reasoning and decision making under uncertainty, network neuroscience, and multi-agent coordination in robotic, power, and transportation networks.

Sylvia Herbert (M'02, SM'06) received her B.S./M.S. degree in mechanical engineering from Drexel University, Philadelphia, PA, USA, in 2014, and the Ph.D. degree in electrical engineering and computer sciences from the University of California, Berkeley, Berkeley, CA, USA, in 2020. She is currently an Assistant Professor with the University of California San Diego, San Diego, CA, USA, where she runs the Safe Autonomous Systems Laboratory. The laboratory uses tools from optimal control theory and dynamics games, machine learning, and cognitive science to develop new safety techniques that are able to quickly adapt to unexpected changes and new information in the system or the environment. She is the recipient of the ONR Young Investigator Award, Hellman Fellowship, UCSD JSOE Early Career Faculty Award, IROS RoboCup Best Paper Award, UC Berkeley Chancellor's Fellowship, NSF GRFP, and the Berkeley EECS Demetri Angelakos Memorial Achievement Award for Altruism